

## REVIEW ARTICLE OPEN

## Flexible inorganic bioelectronics

Ying Chen<sup>1</sup>, Yingchao Zhang<sup>2,3</sup>, Ziwei Liang<sup>2,3</sup>, Yu Cao<sup>2,3</sup>, Zhiyuan Han<sup>2,3</sup> and Xue Feng<sup>2,3\*</sup>

Flexible inorganic bioelectronics represent a newly emerging and rapid developing research area. With its great power in enhancing the acquisition, management and utilization of health information, it is expected that these flexible and stretchable devices could underlie the new solutions to human health problems. Recent advances in this area including materials, devices, integrated systems and their biomedical applications indicate that through conformal and seamless contact with human body, the measurement becomes continuous and convenient with yields of higher quality data. This review covers recent progresses in flexible inorganic bio-electronics for human physiological parameters' monitoring in a wearable and continuous way. Strategies including materials, structures and device design are introduced with highlights toward the ability to solve remaining challenges in the measurement process. Advances in measuring bioelectrical signals, i.e., the electrophysiological signals (including EEG, ECoG, ECG, and EMG), biophysical signals (including body temperature, strain, pressure, and acoustic signals) and biochemical signals (including sweat, glucose, and interstitial fluid) have been summarized. In the end, given the application property of this topic, the future research directions are outlooked.

npj Flexible Electronics (2020)4:2; <https://doi.org/10.1038/s41528-020-0065-1>

## INTRODUCTION

Driven by the desire to better understand the human body, thus keep it healthy, electronics for biomedical applications are developing fast.<sup>1–3</sup> Flexible/stretchable electronics are extending the concept of healthcare in both spatial and temporal dimension by enabling much more accurate and comfortable monitoring and treatment.<sup>4–16</sup> With accurate and massive data measured by the electronic devices that can be integrated with the human body, biomedical applications could ride the tide of artificial intelligence and internet of things.

Basically there are two strategies to realize flexible and stretchable electronic devices. One, known as plastic electronics, is to develop and utilize the intrinsic deformable organic materials with conductivity, semi-conductivity or other properties in transduction and energy storage and so on.<sup>17–22</sup> OLED (organic light emitting diode) display is a successful example for flexible organic electronics. The other is inorganic flexible/stretchable electronics, whose functional elements are based on inorganic materials. By transfer printing, conventional brittle inorganic electronic materials, like silicon, could be transferred into a stretchable and flexible form.<sup>23</sup> The main advantages of the latter are much higher electronic mobility, better stability, much less aging in the air as well as highly mature manufacture technique.

The research interests and products in flexible and stretchable inorganic electronics have been springing up ever since the discovery of stretchable silicon ribbon which was marked as one of the top 10 technologies by MIT's Technology Review Magazine<sup>24</sup> in 2006. Especially in the biomedical field, electronic devices have to be flexible and/or stretchable in order to intimately integrate with the soft, deformable, and configuration-complicated biological tissue.<sup>25–30</sup> Flexibility of the electronic devices can be realized by reducing their thickness, since the bending stiffness decreases at a three orders faster speed with decreasing thickness, while stretchability can be achieved by pre-strain formed wavy configuration, island-bridge structure and serpentine and fractal interconnects design.<sup>23,31–37</sup>

The main idea in these strategies is to utilize the buckling/post buckling of the delicate patterned inorganic materials to minimize the strain in the functional layer while the whole devices are under large deformation. Mechanics analysis, such as FEA (finite element analysis) is very helpful to determine and optimize the stretchability of the device.<sup>33,36,38–44</sup>

Flexible and stretchable inorganic devices' fabrication is generally based on micro-fabrication including film deposition, lithography and most importantly transfer printing technology which transfers the inorganic functional unit from the donor substrate onto the soft target substrate.<sup>45</sup> The typical transfer printing method depends on the kinetic control of elastomeric stamps (e.g., PDMS stamps) whose interface strength towards the inorganic material can be tuned by the peeling speed, contact area or shear stress. In order to transfer and print successfully, this interface strength has to be strong enough to pick the inorganic elements up from the donor rigid substrate yet weak enough to release them onto the target soft substrate.<sup>46–52</sup> Recent years stamps based on shape memory polymer (SMP) have been proposed for scalable, selective, and programmable transfer printing taking the advantages of the reversible adhesion of the SMP.<sup>53,54</sup>

With these design and fabrication strategies for flexible and stretchable inorganic electronics, devices aiming at biomedical applications are now being utilized in the fields range from the monitoring to diagnose and therapy as shown in Fig. 1. The two key considerations for flexible/stretchable devices to measure physiological signals in human body are accuracy and compatibility. As shown in Table 1, the intrinsic challenges for accurate monitoring are low SNR (signal noise ratio) and weak relevance. Conformal contact can be helpful to enhance the SNR of weak signals like EEG.<sup>55</sup> And porous/hybrid electrode can be used to enhance the SNR during sweat composition analysis.<sup>56,57</sup> Building electrochemical channels with ultrathin and conformal electrode has been proved to be an effective way to overcome the weak relevance in chemical signal inside and outside the human body,

<sup>1</sup>Institute of Flexible Electronics Technology of THU, Zhejiang, Jiaxing 314000, China. <sup>2</sup>AML, Department of Engineering Mechanics, Tsinghua University, Beijing 100084, China. <sup>3</sup>Center for Flexible Electronics Technology, Tsinghua University, Beijing 100084, China. \*email: fengxue@tsinghua.edu.cn

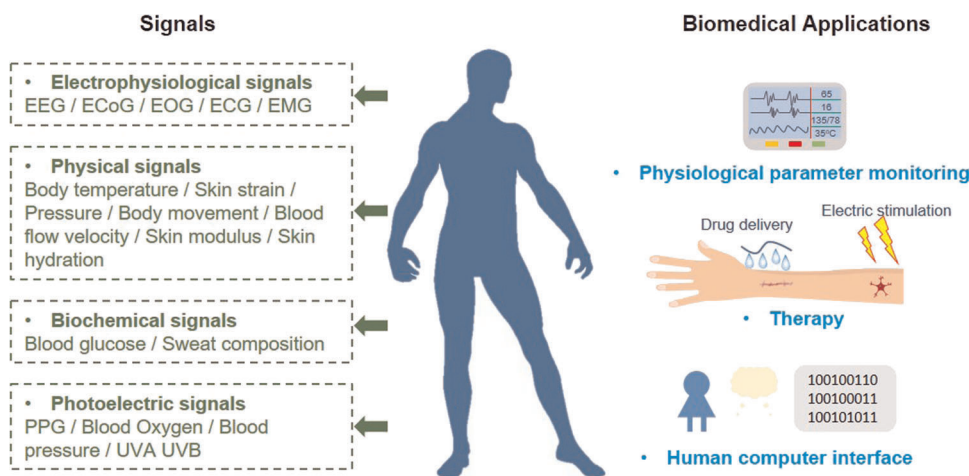


**Fig. 1** Applications that can be realized by integrating biomedical devices onto different parts of human body.

<b>Table 1.</b> Challenges and strategies for flexible/stretchable devices to measure the physiological signals on human body accurately.			
Accuracy and consistency			
Challenges	Example signals	Strategies	Refs
<b>Intrinsic</b>			
Low SNR	EEG	Building conformal and biocompatible neural interfaces	55,96–102,104,105
	Sweat composition	To improve the electrochemical activity of sensors by porous/hybrid electrode	56,57
Weak relevance	Non-invasive blood glucose	Extract glucose from interstitial fluid or blood to the surface of the skin through the method of Electrochemical channels	58
<b>Extrinsic</b>			
Dynamic deformation	Body temperature	Composite materials with zero gauge factor	61
		Rigidity programmable substrate	25
Temperature noise	Sweat composition	Temperature sensor as reference	59
Ambient light noise	Blood oxygen	Opaque encapsulation layer and intimate contact	60,62
<b>Interfacial</b>			
Device internal interface	EMG	Root inspired interlocking layer	30
Human-device interface	Sweat composition	Tattoo-inspired electrochemical sensor to realize intimate contact with the skin	63–68

like measuring the blood glucose non-invasively on the skin.<sup>58</sup> The extrinsic elements that should be considered are the dynamic deformation of the human body as well as the environmental effects like temperature and light.<sup>25,59–62</sup> Besides, the internal interfaces of devices as well as the human-device interfaces are also important in collecting the signal accurately in the long term. Micro-structure enhanced device internal interface and tattoo-like electrode enabled intimate contact are the inspiring solutions to these interfacial issues.<sup>30,63–68</sup>

Compatibility is the other vital part for biomedical devices. Generally, they should be mechanically, biologically, and thermally friendly to human body when collecting signals. Useful strategies have been summarized in Table 2. To be mechanically compatible, the stretchability and conformal contact are the basis for devices to be mechanically invisible to the human body.<sup>69–72</sup> With geometry designed strain limiting substrate, a device that resembles the stress–strain behavior of skin can be safe and comfortable in long-term wearing.<sup>73–75</sup> To be biologically compatible, devices working on the skin shall be breathable with the help of textile/micropores or nanofiber meshed membrane based substrate.<sup>76–80</sup> For implantable devices, tunable degradable substrate and bioresorbable functional materials offer them with

the biocompatibility they need inside the body.<sup>81,82</sup> To avoid rejection is a common task for both inside and outside devices, which is solved by encapsulate them with biocompatible materials like PDMS, silicone, PI (polyimide), hydrogel and silk protein and etc.<sup>55,83–86</sup> Moreover, for special working places like wound, the devices should be inhibitive to bacteria, in such cases silver nanoparticle or nanowire based substrate has been demonstrated to be effective.<sup>87–89</sup> Unlike traditional electronics, stretchable/flexible devices are often supported or encapsulated by bad thermally conductive materials like polymer. Considering the sensitivity of human tissue to temperature rise, the temperature rise of the devices is an inevitable problem, when the heat generation of the devices increases with increasing integration density, especially those with power components. Thermal conductivity enhanced substrate and heat sink have been proposed to solve this problem.<sup>90–95</sup>

Here we review the state of art flexible and stretchable inorganic devices regarding to biomedical applications with special focus on the recent advances in the measurement of a variety of basic physiological signals including bioelectrical signals (e.g., electrocardiograph (ECG), electroencephalograph (EEG) and electromyography (EMG)), biophysical signals (e.g., human body

Compatibility		
Aspect	Strategies	Refs
Mechanically		
Stretchability	Structural geometries design	69
Conformal contact	Ultrathin substrate/microstructure substrate	70–72
Skin-like stress–strain behavior	Strain limiting substrate	73–75
Biologically		
Being breathable	Textile/micropores/nanofiber meshed membrane based substrate	76–80
Bio-degradability	Tunable degradable substrate and bioresorbable functional materials	81,82
No rejection	Encapsulation with biocompatible materials like PDMS, silicone, PI, hydrogel and silk protein and etc.	55,83–86
Inhibition of bacteria	Silver nanoparticle/nanowire based substrate	87–89
Thermally		
Thermal management	Thermal conductivity enhanced substrate, or heat sink	90–95

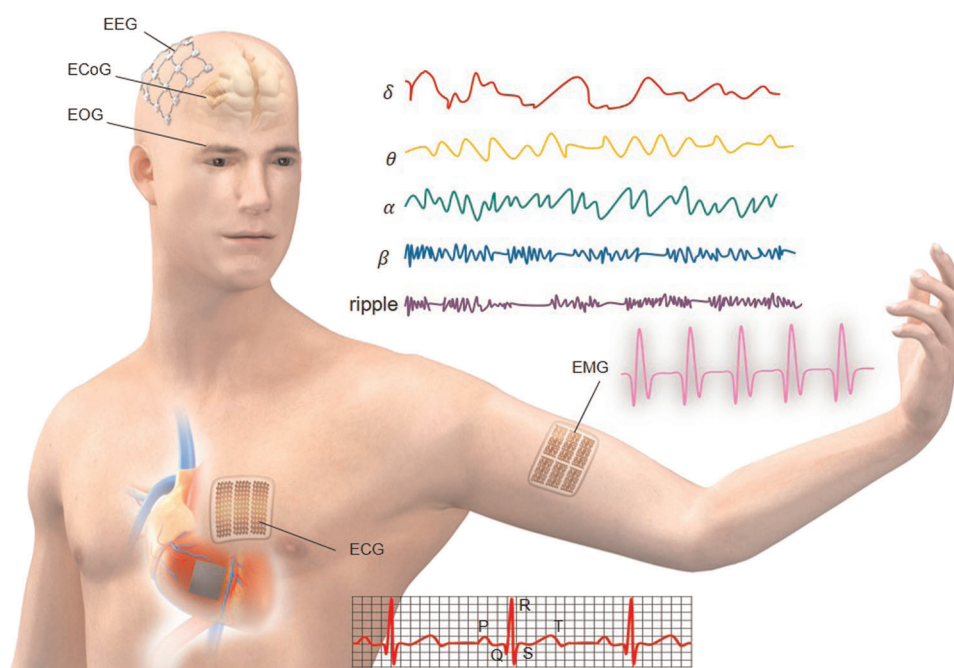


**Fig. 2** Schematic illustration of flexible inorganic electronic devices that are intimately integrated with human tissue for EP signals measuring, including EEG/ECoG, ECG, and EMG.

temperature, strain, pressure, and acoustic signals like heart sounds and bowel sounds) and biochemical signals (e.g., blood glucose and sweat). Since the flexible bioelectronic devices are able to conformal to the curved bio-tissue surface and dynamically adapt to the host's deformation, the SNR and spatial resolution have been much improved compared with (their)the conventional counterparts. Flexible bioelectronics shall not only improve human healthcare but also change our way to study the bioscience.

### BIOELECTRICAL SIGNALS MONITORING

As one of the most important biological signals, the electrophysiological (EP) signals including electroencephalogram (EEG)/electrocorticography (ECoG) of the central nerve system (CNS), action potentials of peripheral nerve system (PNS),

electrocardiogram (ECG), electromyogram (EMG) and electrooculogram (EOG) as shown in Fig. 2, contain vital clinical cues about human physiological activities and various diseases. EP signals have been widely studied from clinical applications to human–machine interfaces. In this section we summarize the recent advances in EP signal recording and applications via flexible inorganic electronics.

#### EP signals of CNS and PNS

EEG and/or ECoG (known as the intracranial electroencephalography, i.e., iEEG), measuring the voltage changes induced by the ionic current within the neurons, has been an important method to understand the brain function in cognitive neuroscience and study the neurological disorders in clinical such as epilepsy, Parkinson's disease and Alzheimer's disease and so on.<sup>96</sup> As shown in Fig. 2, the typical EEG signals can be categorized by frequency

bands from ultraslow to ultrafast, including  $\delta$  (<3.5 Hz),  $\theta$  (3.5–8 Hz),  $\alpha$  (8–13 Hz),  $\beta$  (13–30 Hz),  $\gamma$  (30–80 Hz), and ripples (>80 Hz).<sup>97</sup> Traditionally EEG is recorded by surface-contacting electrodes pads with conductive gel placing on the scalp and ECoG is measured by penetrating microneedles.

Despite of significant success in EEG/ECoG related studies, advances in the EEG/ECoG measuring technology are still demanded in the following aspects: (1) increasing the spatial resolution and the measuring area with high-density electrode array; (2) increasing the signal quality with intimately conformal contact and smaller contact impedance; (3) developing long-term and continuous EEG/ECoG recordings with wireless, energy friendly and biocompatible devices.

Recent advances in flexible electronics have offered promising solutions to the abovementioned challenges. Mechanics theory indicates that the bending rigidity of a device determining its flexibility is inversely proportional to the cubic of its thickness. Therefore, reducing the electrode's thickness becomes the first path towards intimate contact, low impedance and consequently better signals.<sup>98–104</sup> Compared with routine electrodes, flexible and large area devices based on polymer substrate, typically the polyimide (PI), are more attractive due to better contact as well as the ability to record signal in larger areas.<sup>101</sup> The flexible multichannel electrode array based on MEMS with total thickness of 10  $\mu\text{m}$  and as many as 252 channels has been proved to be effective in ECoG recording by *in vivo* testing, even after as long as 4.5 month's implantation.<sup>100</sup> To go beyond the self-supporting thickness limit ( $\sim 10 \mu\text{m}$ ) for a flexible device, the ultra-thin electrode based on dissolvable silk fibroin film is proposed as shown in Fig. 3a.<sup>55</sup> When in clinical use, the device is settled on the corresponding brain area. And then saline solution poured on the device dissolves the silk substrate leaving the ultra-thin electrodes mesh (2.5  $\mu\text{m}$ ) forming highly conformal contact spontaneously with the curvilinear brain tissues driven by the capillary forces as shown in Fig. 3b. The dissolvable silk substrate has brilliantly solved the dilemma of thickness between manipulation and flexibility. And the open mesh geometry further increases the intimacy of the two surfaces. The *in vivo* experiments carried out with comparison of thin film electrode on PI with different thickness indicate that this strategy results in higher SNR with good contact as shown in Fig. 3c.

Mapping large areas of the brain without losing high spatial resolution and conformability is attractive both for the basic neuroscience research and the clinical medicine, and one of the primary issues is the large amount of interconnects. By incorporating silicon multiplexed active transistor, a flexible, high-density electrode array has been developed as shown in Fig. 3d.<sup>105</sup> With this strategy the number of required interconnects for  $n \times m$  electrode array has been reduced from  $2mn$  to  $m + n$ , and the spatial resolution of 360 electrodes has been promoted to sub-millimeter (the electrode size is  $300 \mu\text{m} \times 300 \mu\text{m}$  and the spacing is 500  $\mu\text{m}$ ). With the mechanics analysis guided design and transfer printing featured micro-fabrication technology, the whole device is 25  $\mu\text{m}$  thick with encapsulation ensuring its conformal contact on the cat brain surface as shown in Fig. 3e. What's more, this device is so flexible that can be folded without performance degradation and inserted into the interior of sulci with no damage to the tissue, as in the inset of Fig. 3e, to record more valuable signals. Visual evoked responses have been recorded by the device in the carefully designed visual stimuli, and the signal has been shown in Fig. 3f. Accorded with the expectation, the signals recorded by this device have confirmed the prior knowledge in visual function of the brain.

Apart from the ECoG's information quality, another restriction for electrode device's clinical application, especially the post-procedure monitoring, is the invasiveness and extraction surgery risks. Biodegradable electrodes based on transient electronics technology that can record the electrical activity of the brain like

the normal ones while being able to degrade are promising in the long-term ECoG measurement.<sup>81,106</sup> Figure 3g shows the biodegradable and biocompatible electrodes integrated with a rat's brain, which are stable yet transient in a system-level and controllable way. The transient and flexible ECoG electrodes consist of highly doped silicon nano-membrane as the measurement interface, resorbable PLGA (poly lactic-co-glycolic acid) as the flexible substrate and silicon dioxide as the interlayer dielectric isolating the interconnections from the biofluids as shown in Fig. 3h. And the *in vivo* experiments demonstrate that the chronic recordings can be taken with good biocompatibility through this strategy for as long as 30 days.

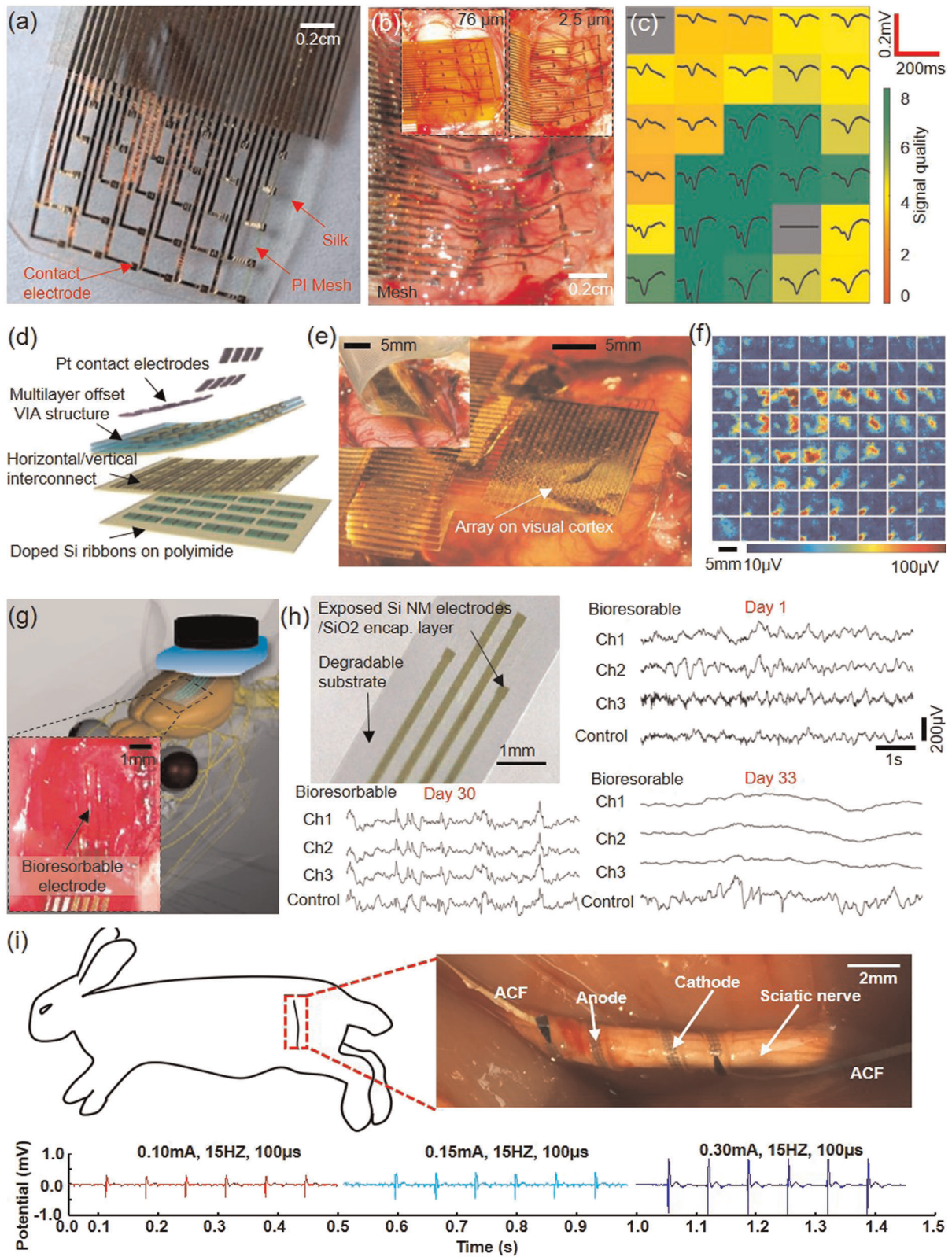
In addition to the recording of CNS, the recording of PNS plays an important role in both neuroscience research and clinical practices.<sup>107</sup> Aiming to balance the invasiveness and high selectivity, researchers have kept optimizing the bio-electrodes for PNS from traditional intraneural electrodes such as Michigan and Utah electrodes, to extraneural electrodes such as cuff electrodes, PI-based electrodes.<sup>108–111</sup> Figure 3i shows a very recently developed 3D twining electrode,<sup>112</sup> which can self-climb onto the peripheral nerve from a two-dimension state with the aid of the shape memory effect. More importantly, the 3D twining electrode can form a flexible and conformal neural interface, which can reduce the inflammation of the nerve tissue without compromising the recording SNR, and it has showed potential in clinical application.

## ECG

Similar to the human brain, flexible inorganic electronics can be used for diagnosing and treating heart disease, such as cardiac arrhythmias and heart failure.<sup>113–116</sup> Lots of work has been carried out to develop flexible electric devices for cardiac electrophysiology mapping and electrotherapy from intracorporal devices such as the balloon catheter and the multifunctional web device that can be conformal integrated with the dynamic heart, to extracorporal devices such as the epidermal electronic system. For the invasive devices, the balloon catheter integrated with ECG multi-electrode arrays, temperature and RF ablation electrodes, is useful for the monitoring of ECG while ablating point by point as shown in Fig. 4a.<sup>117</sup> To further provide full, spatial-temporal cardiac electrical rhythms in real time without manual repositioning like catheter, more advanced multifunctional mapping systems have been developed. Figure 4b shows a conformal, high-density electrodes based on multiplexing circuitry adherent on the cardiac surface with high spatial and temporal resolution.<sup>118</sup> The representative ECG recordings for all 288 electrodes at 4 points in time show that a wave of cardiac activation propagating from the left side of the array to the right side as shown in Fig. 4c.

As for the epidermal electronic system for the ECG monitoring, the capacitive measurement is regarded as the advanced method compared with those in need of contacting gels, due to the advantages such as friendly sterilization, non-currents leakage, less irritation or allergic reactions, and most importantly less sensitivity to motion artifacts.<sup>85</sup> With its flexibility and stretchability the epidermal ECG sensor can be intimately integrated with human body reversely simply by van der Waals force as shown in Fig. 4d. The equivalent circuit model of capacitive ECG sensor is shown in Fig. 4e. The contrast of signal of capacitive flat and rigid electrodes to that of the epidermal ECG sensor shown in Fig. 4f demonstrates the ability of the latter to resist the artifacts caused by motion.

Cardiac electrotherapies, which include cardiac ablation therapy, pacing and defibrillation, play critically important roles in treating cardiac arrhythmias. Lots of effort has been made to diminish the interface mismatch between the electrodes and the cardiac tissue by adopting the strategies and technologies of the flexible inorganic electronics. The abovementioned balloon



catheter integrated RF electrodes cloud provide precise access to anatomical regions to ablate abnormal focal tissues.<sup>117</sup> Development of flexible and stretchable electrodes with large coverage area (i.e., mesh electrodes) will benefit the cardiac pacing and defibrillation where large areas of the myocardium are required to be excited simultaneously.<sup>115,119–121</sup> In the meantime, the

flexibility and stretchability of the mesh electrodes not only largely reduce the effective modulus of the whole devices and guarantee that the cardiac will not bear large pressure, but also increase the mechanical reliability so that the electrodes could deform compatibly with the dynamically beating heart.

**Fig. 3 Flexible electrodes for EP signals recording of PNS and CNS.** **a** Completely conformal electrode array for the mapping of ECoGs; **b** image of the electrode array (25  $\mu\text{m}$  mesh) on a feline brain after the dissolve of the silk substrate. Inset, 76 and 2.5  $\mu\text{m}$  electrode arrays; and **c** the recorded ECoG with the color showing the SNR. **d** The structure of the flexible, high-density electrode array with high spatial resolution and large coverage; **e** the image of the high-density electrode on a cat brain for the mapping of the visual cortex; and **f** the visual evoked response of the 360-channel electrode array. **g** Biodegradable electrodes integrating on a rat's cortical surface; and **h** the structure (upper middle) and in vivo chronic recordings of the rats with a duration of about 30 days (down middle and right). **i** 3D twining electrode for peripheral nerve system. **a–c** Reproduced with permission<sup>55</sup> (Copyright 2010, Nature Publish Group). **d–f** Reproduced with permission<sup>105</sup> (Copyright 2011, Nature Publish Group). **g, h** Reproduced with permission<sup>81</sup> (Copyright 2016, Nature Publish Group).<sup>112</sup> (Copyright 2019, American Association for the Advancement of Science).

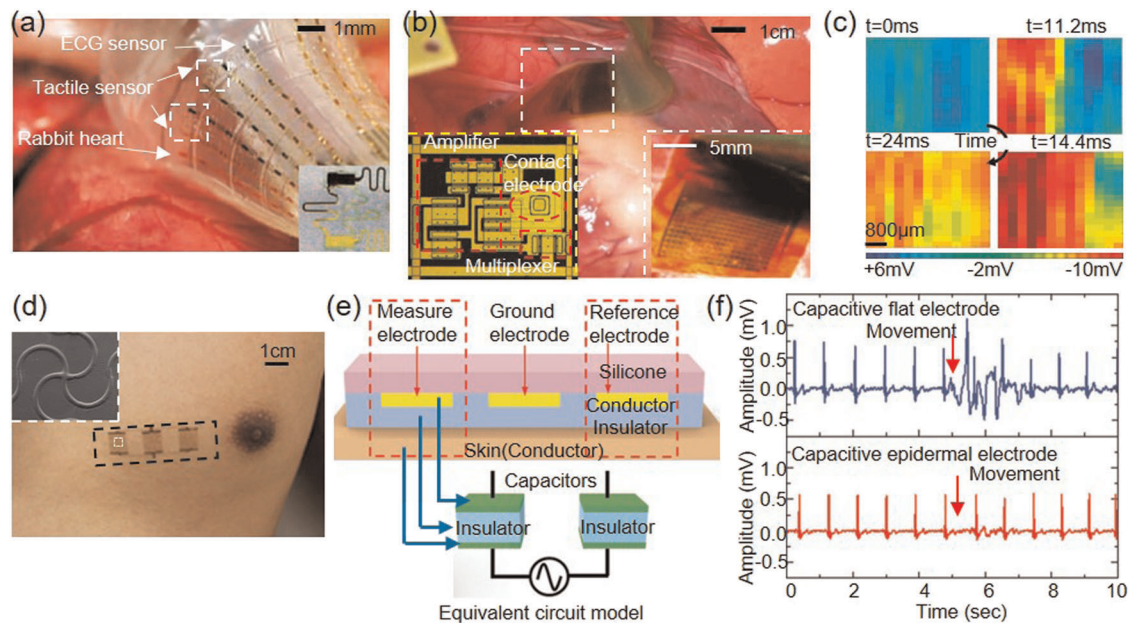


**Fig. 4 ECG measurement by flexible devices.** **a** Balloon catheter for the cardiac electrophysiological mapping and ablation therapy. **b** The image of the high-density electrodes on a porcine heart for the recording of the spatial-temporal cardiac electrical rhythms in real time, the inset shows the circuit unit and the enlarged view of the electrode array; and **c** the recorded wave of cardiac activation propagating of the entire 288-electrodes. **d** The image of the epidermal electronic system on the human skin for the ECG measurement, the inset show the enlarged view of the mesh design; **e** equivalent circuit model of the epidermal electronic system; and **f** comparisons of the ECG recordings with traditional flat electrode. **a** Reproduced with permission<sup>117</sup> (Copyright 2011, Nature Publish Group). **b, c** Reproduced with permission<sup>118</sup> (Copyright 2010, the American Association for the Advancement of Science). **d–f** Reproduced with permission<sup>85</sup> (Copyright 2014, Wiley-VCH).

## EMG

EMG is the recording of the electrical activity generated by the skeletal muscles, which is of critical value in clinical and scientific aspects. Clinically, EMG can be used to evaluate neuromuscular function especially for patients with stroke or Parkinson's disease. Scientifically, EMG can be used to study the muscle pain mechanism or to develop human-machine interface. Generally, EMG can be divided as surface EMG (i.e., sEMG) and intramuscular EMG. The stretchable and flexible EMG sensors that can be integrated with the epidermis or skeletal muscles are desired due to much smaller and more stable interface resistance, especially with the good performance during dynamic measurement.

Several epidermal devices have been introduced to measure the sEMG.<sup>83,122</sup> Figure 5a shows such an epidermal EMG sensor that wears on human body.<sup>83</sup> An EMG sensor (including the measurement, reference and ground electrode), a temperature sensor, a strain gauge as well as several stimulation electrodes are integrated on the device. The temperature sensor measuring the skin temperature can be helpful in muscle fatigue detection. And the strain gauge measures the deformation of the muscle. The structure of the integrated device is simple. It is consist of three layers of insulating polyimide and two layers of metal traces, i.e., one is the measuring layer and the other is the stimulating layer. To demonstrate the performance of both the sensing and

stimulating electrode, the M-wave signal was recorded with 1 Hz and 50 V stimulation, as shown in Fig. 5b.

The devices measuring intramuscular EMG signals have been reported by Kim et al.<sup>123</sup> Researchers developed a stretchable and transparent cell-sheet-graphene hybrid device comprised of biocompatible materials whose layout is shown in Fig. 5c. The Au-doped graphene mesh in the device served as the recording and electrical stimulating electrode. Not only can recording the EMG signal, this device can also benefit the wounded muscle in regenerating the cell sheets by applying electrical stimulation, as demonstrated in the in vivo testing shown in Fig. 5d, e.

What's more, combining the electrode stimulating function in EMG devices with EP recording function in EEG/ECoG devices, neuromuscular electrical stimulation can be designed to form an electronic neuroprosthetic device for paralysed human to control machines like computers and robotic arms through thinking. This device acts as the signal pathways between the brain and the muscles. Bouton et al. proposed a prototype in which the ECoGs can be linked in real time to muscle activation as shown in Fig. 5f.<sup>124</sup> They decoded the neuronal activity from the ECoGs through machine-learning algorithms and then restored movement by applying high-resolution neuromuscular electrical stimulation. As the ending of this section, this work has pictured an exciting image where brain cannot only control the healthy body, but also the disabled human body or even machine, which shall be

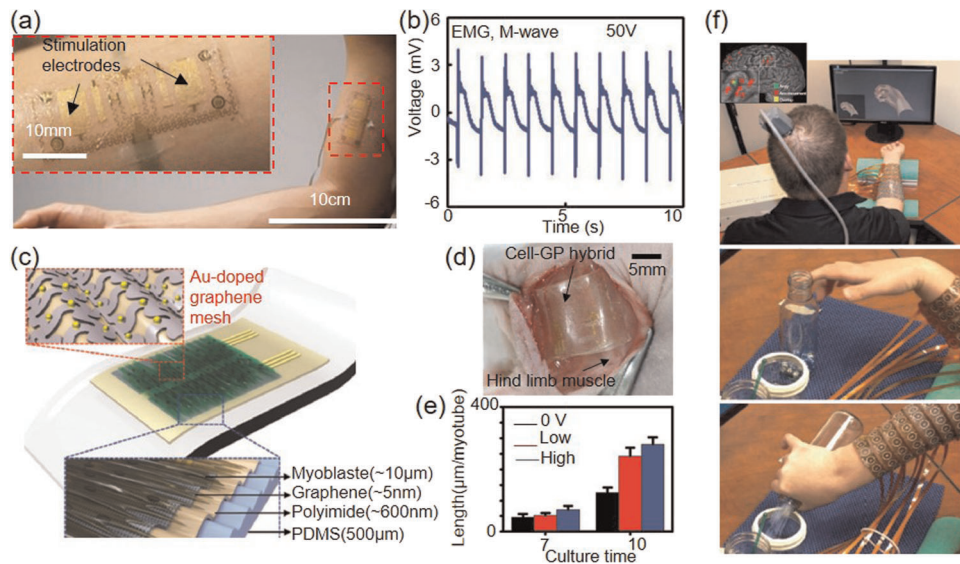


**Fig. 5** Flexible devices that can measure EMG signals, and build the neural bypass. **a** The image of the epidermal EMG sensor on the human biceps for the neuromuscular electrical stimulation therapy and function diagnosing; and **b** the evoked M-waves of the biceps during 1 Hz stimulation at 50 V. **c** Stretchable and transparent cell-sheet-graphene hybrid for recording EMG signals and therapy of the skeletal muscle; **d** the image of the hybrid implantation onto target muscle; and **e** the length of the myotube at day 7 and day 10 under different voltage (down right). **f** Neuroprosthetic devices for the restoring lost motor function. Experiments of decoding ECoGs (upper), and functional movement task (middle and bottom). **a, b** Reproduced with permission<sup>83</sup> (Copyright 2015, Wiley-VCH). **c–e** Reproduced with permission<sup>123</sup> (Copyright 2016, Wiley-VCH). **f** Reproduced with permission<sup>124</sup> (Copyright 2016, Nature Publish Group).

realized by the stretchable and flexible EP sensors in the near future.

### BIOPHYSICAL SIGNALS MONITORING

Attaching the flexible biomedical devices on the skin can measure the biophysical signals of human body, such as temperature, strain and pressure. Among them, temperature is one of the fundamental parameters most concerned by the physicians. Continuous and long-term monitoring of basal body temperature, local temperature around the wounds, as well as the skin temperature mapping near the superficial blood vessel gives important hint for the clinical diagnose. Moreover, strain and pressure on the human body can be used to reflect all kinds of physiological activities that cause tissue's deformation, such as body movement, pulse, respiration and phonation. Herein, various skin-like devices have been developed to measure the temperature, strain and pressure of human body by integration with the skin. The main challenges regarding to these skin-like devices are (1) the biocompatibility issue concerning long-term integration with human skin; (2) decoupling the noise caused by body movement from the subtle signal of interest; (3) to integrate more functions in a single device, and so on. As shown in Fig. 6a, these skin-like devices have been applied in various scenarios like wounds monitoring and therapy, blood flow sketching and skin status assessment, and so on. This section introduces strategies to measure temperature, strain and pressure of human body by integrating flexible and stretchable devices onto the skin, with emphasis on the abovementioned challenges as well as the applications.

#### Body temperature

A variety of flexible temperature sensors have been developed to measure body temperature. The measuring materials commonly used are metal,<sup>125</sup> semiconductor,<sup>126</sup> carbon group materials,<sup>127,128</sup> polymer-carbon group materials composite<sup>129</sup> and the thermochromic liquid crystals<sup>130</sup> and so on. Regardless of all kinds of sensitive materials and sorts of device design in flexibility and stretchability, for devices aiming at measuring body temperature

in long-term and continuous style, the priority faced with them is the compatibility issue raised by the allergy or infection of the skin. And the allergy is the result of skin's failing to breathe. Although the skin's breathing contributes little to the whole body, the cells located within 0.25–0.4 mm to the skin surface are heavily relied on this activity.<sup>131</sup> As shown in Fig. 6b, a breathable and stretchable temperature sensor inspired by skin is realized by introducing porous structures, as shown in the SEM image in the inset, into the substrate and encapsulation layer of the device.<sup>80</sup> With pore sizes ranging from a few tens of nanometer to several micrometer, the substrate and encapsulation layers are permeable for the sweat to go through in the form of water vapor to avoid maceration and air (such as oxygen and carbon dioxides) to get in and out for breathing. Together with the serpentine like function layer, the whole device is breathable and stretchable just like the human skin. The in vitro test shows that after 24 h wearing including two times of shower (shown in Fig. 6c), the skin under the device exhibits no sign of maceration or stimulation (shown in Fig. 6d). Besides, as shown in Fig. 6e, the accuracy of this device is comparable to that of the mercury thermometer in axillary's temperature (i.e., the underarm temperature) measuring.

The utilization of soft materials enables flexible sensor conformally integrated with human epidermis; in the meanwhile, inevitable deformation of skin also brings deviation into real-time measurement due to the strain-resistive behavior. Several strategies have been proposed to diminish this strain caused noise to temperature signal. Solutions include design in structures, thermal sensitive materials as well as in fabrication strategy. Strain limiting substrate, by integrating rigid thin film onto pre-strained substrate to form wavy like composite substrate, is one of the structure design solutions.<sup>73</sup> To place sensitive elements on the neutral layer or micro-patterns,<sup>132</sup> where the strain is nearly none or isolated from the substrate, are also effective structure designs. Besides, encapsulating the sensitive elements in liquid environment, so that the elements can be detached from the substrate to buckle freely with much smaller strain, is also able to diminish the strain noise.<sup>133</sup> From the aspect of materials science, the best solution to this strain noise is to develop sensitive materials that is

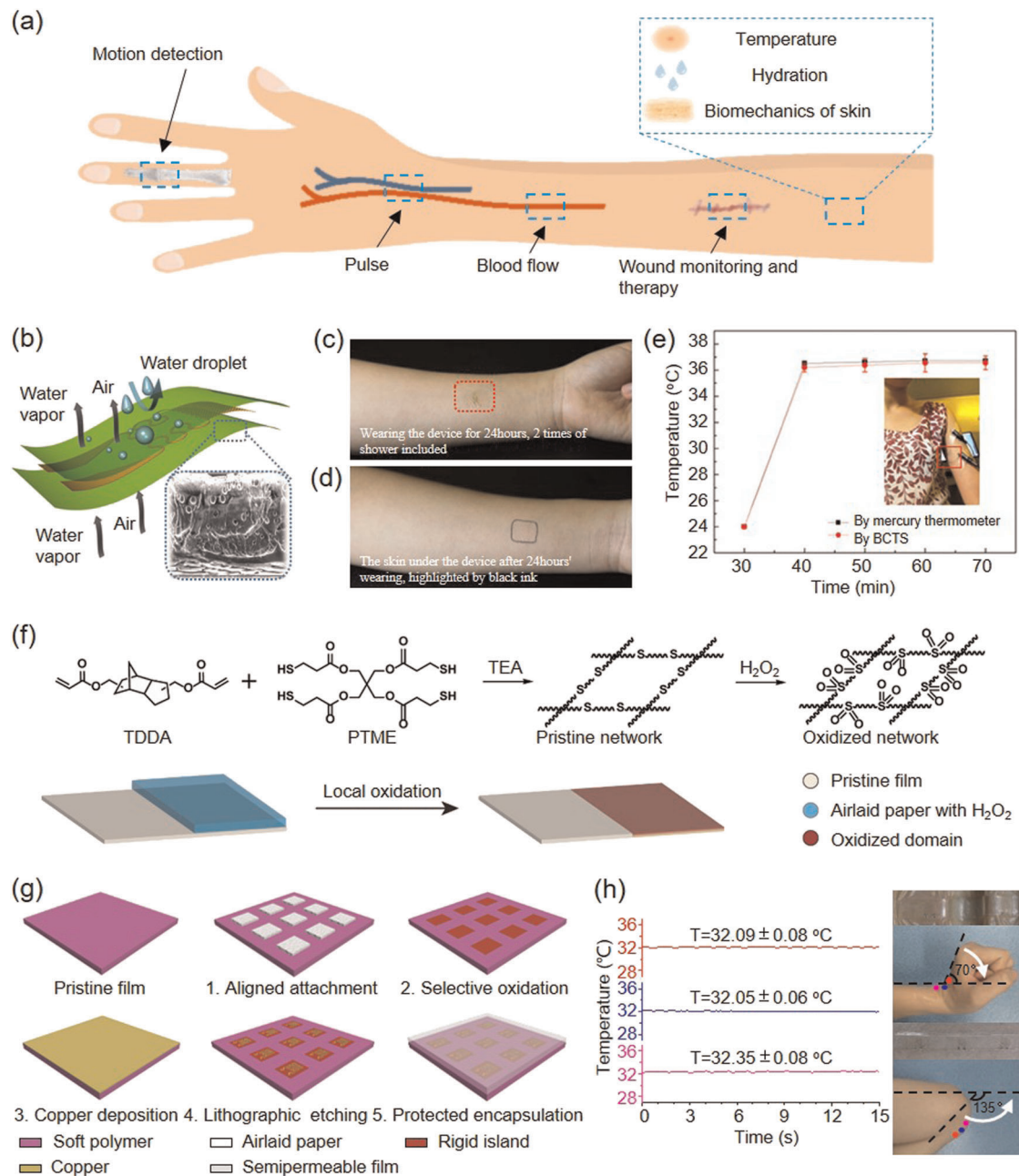


**Fig. 6 Temperature monitoring for human body.** **a** Applications of flexible devices upon human skin. **b** The illustration of water proof and vapor permeable property of the sensor; **c** wearing the sensor for 24 h with two times of shower; **d** the skin under the device after 24 h' wearing, no sign of maceration or stimulation is observed; and **e** in vitro test of the sensor and its comparison with the mercury thermometer. **f** Synthetic scheme of the thiol-acrylate-based polymer and its chemical modification via oxidation (top), spatio-selective oxidation (bottom); **g** device fabrication flow chart; and **h** real-time temperature measurement corresponding to fast (1 Hz) wrist movement (left), the temperature sensor array placed on wrist and knee (right). **b–e** Reproduced with permission<sup>80</sup> (Copyright 2015, Nature Publish Group). **f–h** Reproduced with permission<sup>25</sup> (Copyright 2018, Wiley-VCH).

only sensitive to temperature, yet insensitive to strain, i.e., the gauge factor (GF) is zero. This kind of materials has been obtained by forming composite polymer with positive and negative GF materials in certain proportion, thus the composite polymer's GF is zero.<sup>61</sup>

However, the structure designs can reduce the strain in the functional layer to a large degree, yet fail to fully diminish the strain. Besides, when in actual applications, the abovementioned strategies all have their limitations. The neutral layer's position may deviate at different level when the device is attached onto human skin. The micro-patterns, strain limitation structures as well

as liquid encapsulation may increase the thickness of the substrate to some degree, thus decrease the flexibility of the whole device. And the composite materials method is limited to certain polymer, which is unfriendly to the inorganic flexible electronics. Therefore, rigidity programmable substrate based fabrication method is proposed.<sup>25</sup> The chemical principle of this rigidity programmable substrate is shown in Fig. 6f. The pristine material, namely the polysulfide elastomer originates from thiol-acrylate click chemistry, and its rigidity can be regulated through oxidized chemical modification of hydrogen peroxide (H<sub>2</sub>O<sub>2</sub>). The fabrication strategy is demonstrated in Fig. 6g. The spatio-selective oxidation

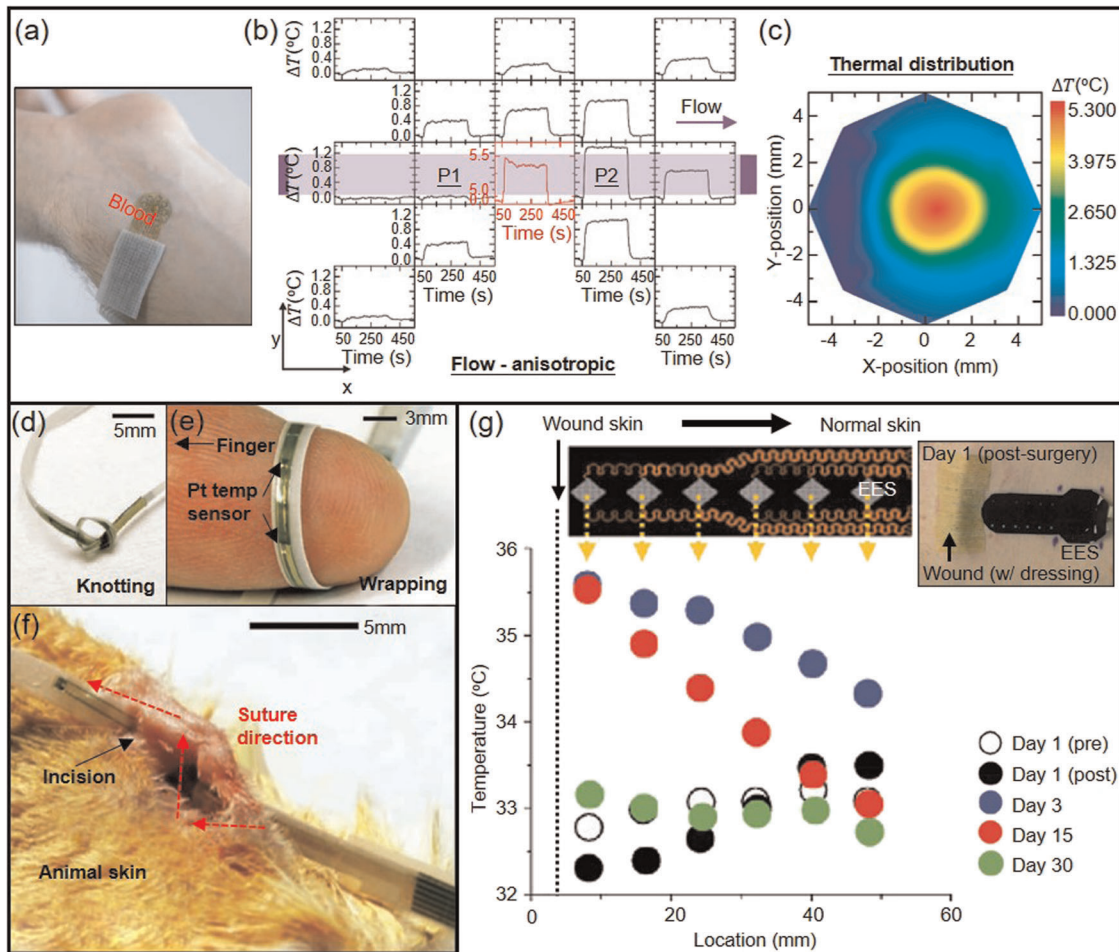


**Fig. 7 Measurement of blood flow and monitoring of wound healing.** **a** Photograph of a device on the skin; **b** raw data from a device applied to an area above a large vessel; and **c** spatial map of the temperature at  $t = 300$  s. **d** Optical image of a suture strip after knotting; **e** example of a device under wrapping; and **f** temperature monitoring using an instrumented suture strip at the location of an incision on an animal model. **g** Photo of the wound with an EES on day 1 (higher right), temperature distribution recorded with an EES over the course of one month after the surgery. **a–c** Reproduced with permission<sup>134</sup> (Copyright 2015, the American Association for the Advancement of Science). **d–f** Reproduced with permission<sup>126</sup> (Copyright 2012, Wiley-VCH). **g** Reproduced with permission<sup>135</sup> (Copyright 2014, Wiley-VCH).

is introduced by patterned airlaid paper to enhance local rigidity that is capable of strain-isolation resorting to the ultra-large contrast of modulus ( $\sim 150$ ). This critical step makes this direct fabrication eligible to adapt to well-established lithographic process. Thus, functional elements like temperature sensor array can be directly fabricated upon the treated substrate with the units located on rigid regions. To evaluate its effectiveness, the device is placed on both wrist and knee joints undergoing large and dynamic deformation. All sensing units report highly constant temperature values with variation less than  $0.08$  °C regardless of the motion frequency as shown in Fig. 6h, thus indicating the validity of this simple method in strain isolation.

#### Blood flow

Other than body temperature, skin-like devices can also play important if not revolutionary role in blood flow and wound monitoring applications. Take blood flow as an example, traditional measuring methods are faced with a common dilemma hindering the accuracy. Specifically, to guarantee the accuracy, the devices need to be pressed onto the human body to form good contact, yet this pressure will change the blood flow locally; and the non-contact measurements are always quite sensitive to motion and deformation of human body.

Skin-like devices can solve this difficulty since they can work on the skin in a mechanically invisible way with good accuracy even in condition of body movement or deformation. Epidermal devices based on thermal principle have been studied to map the blood flow in a non-invasive, precise and continuous way.<sup>130,134</sup> Gao et al.<sup>130</sup> introduced an ultrathin, skin-like photonic device for mapping thermal characteristics of the skin. They patterned the thermochromic liquid crystals into large-scale, pixelated arrays and placed them on thin elastomeric substrates as colorimetric temperature indicators. Through analysis of spatio-temporal images obtained from radio frequency (RF) components, thermal conductivity and thermal diffusivity are accurately measured with milli-Kelvin precision ( $\pm 50$  mK) and sub-millimetre spatial resolution. Their demonstrations in the reactive hyperemia assessments of blood flow and hydration analysis, related to cardiovascular and health skin-care respectively, highlight the application in clinically meaningful tests. As shown in Fig. 7a, Webb et al.<sup>134</sup> reported an epidermal device for continuous mapping of macro-vascular and micro-vascular blood flow based on the anisotropic thermal transport phenomena around subsurface blood flow region. The device consists of a metallic thermal actuator, served as a constant source of thermal power to create a well-controlled increase in temperature, and 14 resistive sensors for sensing the spatiotemporal distributions of temperature that

result from the heating. During measurement, the thermal distribution is strongly anisotropic, and the bias indicates the blood flow behavior, as shown in Fig. 7b, c. The device platform naturally conforms to the surface of the skin to eliminate relative motion between the actuator/detectors and blood, allowing for precise blood flow mapping as indicators of vascular health, particularly in diseases with vascular-associated pathologies.

#### Wound monitoring

The advantage of flexible and stretchable devices in wound monitoring is to get quantitative assessment of the local tissue during the wound's healing process. As shown in Fig. 7d–f, a flexible smart surgical suture has been designed and fabricated, which is integrated with silicon nanomembranes (Si NM) diode temperature sensors and microscale Joule heating elements for sensing and potential programmable delivery of local heating and electrical stimulation to promote healing of chronic wounds.<sup>126</sup> The device exploits biocompatible materials such as silicon in nanomembrane formats coordinated with natural biological responses in the body for improved health outcomes. The application of this smart surgical suture in *in vivo* animal experiments provides evidence for the practical use of this new class of devices.

Moreover, an integrated biomedical device has been developed as shown in Fig. 7g, and it incorporates six micro-metal resistors/actuators for precise time-dependent mapping of temperature and thermal conductivity of the skin near the wounds with precision about 50 mK.<sup>135</sup> The use of biocompatible, ultra-soft layers of silicone, serving as the encapsulations, is capable to enhance the wearability on hypersensitive wound tissues, simple procedures for disinfection as well as the re-use property.

#### Strain and pressure

Another critical parameter that can be measured on the skin is the active or passive deformation, namely the strain or pressure, resulted from the motion or certain physiological activity, from which we are able to detect body movement, pulse, respiration, pronunciation and the mechanical property of skin and so on.<sup>136</sup> For both strain and pressure measuring, there are resistive, capacitive, piezoelectric and triboelectric sensors and so on. The resistive functional materials include metal thin film,<sup>137,138</sup> metal nanomaterials,<sup>139–142</sup> liquid metal,<sup>143,144</sup> carbon nanotube,<sup>145–149</sup> graphene,<sup>150–154</sup> carbon black<sup>155,156</sup> and so on.

When applied on human body, different measuring objects require the device's stretchability, sensitivity, linearity, detection range and detection limit differently. To match these requirements, functional material's category, pattern as well as the micro structures of the device can be considered. Usually measuring the joints' movement requests the sensor to be highly stretchable, dynamically responsive and reliable with large detection range since the deformation is relatively large. Therefore, non-metal materials are good choices. As shown in Fig. 8a, Yamada et al.<sup>157</sup> reported a strain sensor based on aligned single-walled carbon nanotubes (SWCNT) capable of measuring strains up to 280%, with high durability, fast response and low creep. Under stretching, the SWCNTs fracture into gaps and islands with bundles bridging the gaps, which causes relative change in resistance serving as a quantitative index. Applications of detecting movement, typing, breathing and speech by incorporating into clothing or attaching directly to the body have been demonstrated. And the collective results suggest a wide prospect in recreation, virtual reality, robotics and healthcare.

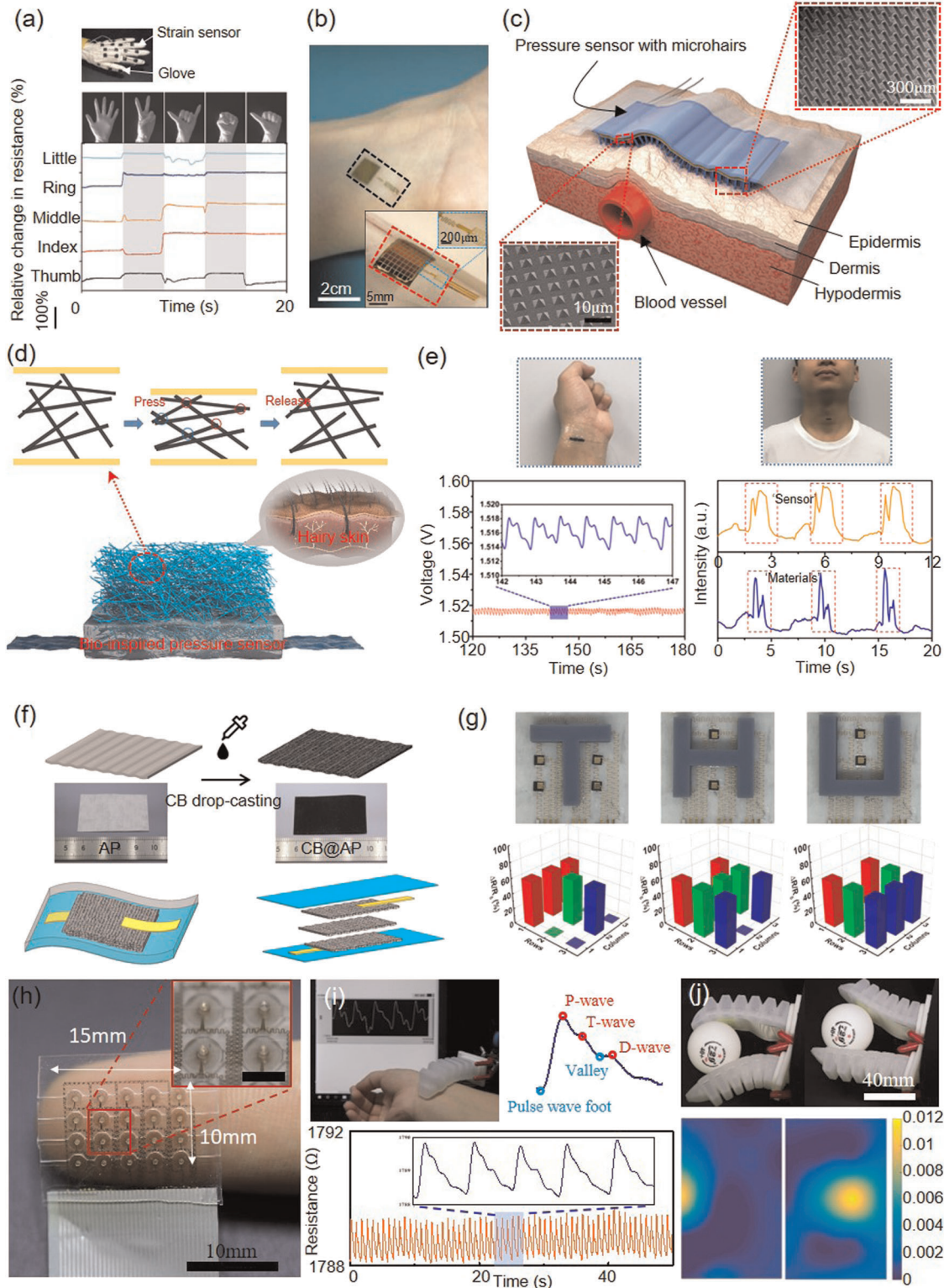
On the other hand, for weak activity monitoring like pulse or respiratory, it is better that the sensor is highly sensitive and mechanically invisible with small detection limit. Specifically, the large sensitivity and small detection limit are to deal with the subtleness of these signal, while the mechanical invisibility is to

avoid any disturbance caused by the sensor itself. Therefore, metal or piezoelectric sensors are preferred from the perspective of materials. As shown in Fig. 8b Dagdeviren et al.<sup>158</sup> exhibited a piezoelectric sensor based on lead zirconate titanate (PZT) with enhanced piezoelectric response for cutaneous pressure monitoring whose sensitivity is  $\sim 0.005$  Pa and the response time is  $\sim 0.1$  ms. To amplify the response, the capacitor-type structure PZT is connected to the gate electrodes of MOSFETs based on nanomembranes of silicon (SiNMs). And the applications include arterial pulse pressure wave and speech caused motion on the throat measurements are demonstrated to indicate the feasibility of using flexible devices to measure the subtle signals on human body.

In addition to highly sensitive materials, micro-structures design is another important strategy to obtain highly sensitive sensors, especially with non-metal materials.<sup>72,156,159–167</sup> Various bio-inspired micro-structures are the typical ones. Take one as an example, the bioinspired microhair interfacial structures are introduced in a wearable bandage-like capacitive pressure sensor to amplify the weak pulse signals, as shown in Fig. 8c.<sup>72</sup> It is observed that the SNR has been substantially improved comparing to that with flat device with no microstructure. Moreover, they demonstrate that the waveforms retrieved from a healthy subject and a person with cardiac diseases show different patterns, suggesting that the device can be advantageous toward expeditious diagnosis of cardiovascular and cardiac illnesses.

Another type of micro-structures design is based on 3D porous conductive network, such as carbon black-polyurethane (PU) sponge,<sup>156</sup> carbon nanotube-polymer sponge,<sup>168</sup> carbon aerogels<sup>169</sup> and etc. The porous structures based sensors are widely applied in pressure sensing and other various applications because of their high sensitivity, ultra-light weight, high porosity and other versatile properties. Currently there are two main strategies to form the 3D porous conductive network. One is to coat conductive materials on polymer based sponge, and the other is to directly build the conductive network with conductive materials, such as carbon fibers. A carbon black-PU sponge based pressure sensor, whose sensitivity is  $0.068$  kPa<sup>-1</sup>, is the represent of the former strategy.<sup>156</sup> When the 3D porous materials are combined with bio-inspired structures, the device's sensitivity can be further improved. Han et al. reported a flexible skin-inspired pressure sensor based on 3D carbon nanofiber networks (CNFNs) as shown in Fig. 8d.<sup>27</sup> The results show that this device not only possesses higher pressure-sensitivity ( $1.41$  kPa<sup>-1</sup>), but also exhibits stable resilience and super compressibility (>95%), due to the nano-reinforcement of Al<sub>2</sub>O<sub>3</sub>. Similar to that of other conductive network based sensor, the pressure measurement principle is demonstrated in Fig. 8d, namely the resistance of the network is determined by the pressure controlled conductive path. Inspired by the hairy skin, part of the network is imbedded in the polymer substrate while the other is free in the air. Thus, the exposed CNFNs corresponding to hair can detect tiny movement and air blow while the infiltrated section corresponding to skin can increase the mechanical stability. The electrodes corresponding to nerve can transmit electric signals. As shown in Fig. 8e, the sensor is sensitive enough to precisely monitor human physiological signals, including phonation, pulse, respiration and joint's movements, which indicates promising applications in healthcare and human-machine interaction.

For flexible strain/pressure sensor, the ultimate goal is to be applied in daily life. Therefore, in addition to excellent performances, low cost and simple preparation process are also of great importance for the sensors to have practical applications in real life. Recently, Han et al. reported an ultralow-cost flexible pressure sensor based on carbon black (CB) and airlaid paper (AP).<sup>170</sup> Compared with well-studied sensing materials, such as graphene, rGO (reduced graphene oxide), and Au/Ag nanowires, conductive CB and AP are ultra-cheap raw materials. The sensing materials are



just prepared through drop casting CB solutions onto APs (Fig. 8f top) following by stacking multilayer CB composites (Fig. 8f down). The simply fabricated sensor has ultrahigh sensitivity of  $51.23 \text{ kPa}^{-1}$ . Except for human physiological signals monitoring, the sensor could be integrated into a flexible array electronic skin (Fig. 8g) for spatial pressure distribution detecting.

Beside the application of directly monitoring physical signs of human by integrating with skin, flexible strain/pressure sensors

are also could be used to realize the intelligent haptic perception of robotics, which will make great significance on medicine and artificial limbs. Liang et al. proposed a new kind of high-performance flexible tactile sensor and sensor array based on photolithography and etching technique as shown in Fig. 8h.<sup>171</sup> By integrating the tactile sensor on the surface of a soft prosthetic hand, the smart hand could complete various tasks like a real hand, including imitating the process of traditional Chinese

**Fig. 8 Flexible pressure sensors for detections of motion, pulse and biomechanics of skin.** **a** A strain sensor fixed to a data glove (higher left), relative changes in resistance versus time for data glove configurations. **b** Photograph of a device laminated on a wrist and a device wrapped on a cylindrical glass support (inset). **c** Schematic illustration to detect pulse on a human's neck with a microhair sensor. **d** Schematic illustration of the working mechanism of piezoresistive CNFNs and the pressure sensor, which is bio-inspired by human's hairy skin. **e** Photographs of CNFNs sensor attached onto the wrist to detect the pulse and fixed onto the human neck to identify voice. **f** Preparation process for CB@AP composites (top), and schematic illustration of the flexible multilayer CB@AP pressure sensor. **g** Array electronic skin for spatial pressure distribution. **h** The photograph of the sensor array, the scale bar of inset is 2 mm. **i** The process of pulse detection by a soft prosthetic hand integrated with the tactile sensor and the detected pulse signal. **j** The pressure distribution at different moment when two soft hands rolled a ping pong ball. **a** Reproduced with permission<sup>157</sup> (Copyright 2011, Nature Publish Group). **b** Reproduced with permission<sup>158</sup> (Copyright 2014, Nature Publish Group). **c** Reproduced with permission<sup>72</sup> (Copyright 2015, Wiley-VCH). **d, e** Reproduced with permission<sup>27</sup> (Copyright 2019, the Royal Society of Chemistry). **f, g** Reproduced with permission<sup>170</sup> (Copyright 2019, American Chemical Society). **h–j** Reproduced with permission<sup>171</sup> (Copyright 2019, WILEY-VCH).

medicine pulse diagnosis to detect pulse signals in radial artery, as shown in Fig. 8i and provide real-time spatial distribution of pressure during grabbing objects as shown in Fig. 8j.

### Acoustic signals

Flexible acoustic electronics with acoustic signals from human bodies as detection object is an important contribution to the development of flexible electronics. Generally, there are two types of flexible acoustic devices. One, usually called as flexible acoustic sensors or microphones, senses the vibrations on the skin surface generated by human organs or tissues, such as heart and throat. The time and frequency domain characteristics of sound signals are determined by the characteristics of vibration source as well as the medium, reflecting health status of corresponding organs or tissues. A representative flexible microphone was invented for seismocardiography and heart murmur monitoring as shown in Fig. 9a.<sup>172</sup> The flexible sensor is integrated with a MEMS accelerometer with low-modulus elastomeric encapsulation. It can simultaneously measure heart sounds and ECG signals by adding a pair of capacitive electrodes as shown in Fig. 9b. Heart murmurs are detected by measuring at tricuspid and pulmonary sites of a subject with mild tricuspid and pulmonary regurgitation, which illustrates the sensor's utility in cardiovascular diagnostics. Bowel sounds are also important, for their clinical correlations with intestinal function.<sup>173</sup> Wang et al.<sup>174</sup> have developed a flexible wearable wireless device for long-term and real-time monitoring of bowel sounds, which transmits the sound signal to the mobile handset through Bluetooth by waveform display as shown in Fig. 9c. It includes a 3D-printed elastomeric resonator for the improvement of acoustic sensing. Clinical tests have been conducted with a healthy volunteer and patients with mechanical intestinal obstruction or paralytic ileus, which demonstrates that the device is capable to capture the characteristics of bowel sounds as shown in Fig. 9d. Furthermore, due to its flexibility and portability, a nearly five-hour measurement was applied to monitor the bowel sounds of a subject after meal as shown in Fig. 9e. It turns out that the device can serve as a reference for possible applications of the system in the auxiliary diagnosis of bowel problems.

The other type of flexible acoustic electronics is based on ultrasound applications. Ultrasound is noninvasive and generally regarded as a safe monitoring method for human body. Compared with biochemical and deformation signals, ultrasound can penetrate into human body with large depth. However, the flexible ultrasound device for biomedical applications is only researched in recent years. A flexible and stretchable ultrasound array for continuous monitoring of central blood pressure was proposed in 2018 as shown in Fig. 9f.<sup>175</sup> By using of a 1–3 piezoelectric composite with a working frequency of 7.5 MHz and “island-bridge” layout, the overall thickness of the device is only 240  $\mu\text{m}$ , and it can penetrate the depth of 4 cm under the skin. By measuring the echoes of the anterior and posterior walls of the pulsating blood vessels, the diameter of the blood vessels can be

obtained as shown in Fig. 9g, and then it can be translated into blood pressure. The results of blood pressure in different arteries are in accord with those of commercial tonometer as shown in Fig. 9h. This work combines flexible electronics with ultrasound technology, achieving both wearability and high tissue penetration ability for nondestructive long-term monitoring of human deep tissues.

### BIOCHEMICAL SIGNALS MONITORING

The chemical elements in human body are important and direct indicators of human health. The clinical diagnosis and detection of many diseases needs to retrieval blood sample or other biological fluids for analysis, which may involve physical trauma and bring the risk of infection yet just reflect one single physical condition on the time line. “Finger-pricking” in glucose monitoring for diabetics is a typical example. In order to trace the fluctuation of glucose level at different moment, it needs to be conducted repeatedly for multiple times throughout the day, which brings both physical and emotional pain to the patients. As the flexible electronics technology develops, the demand of wearable medical devices for remote medicine and chronic disease management at home is also increasing. As the alternatives or complements to blood, other more accessible biological fluids such as sweat, interstitial fluid (ISF), saliva, ocular fluid or urine also contain a lot of useful information for non-invasive continuous health monitoring. All of those leads to the progress of flexible electrochemical sensors for non-invasive or less invasive continuous monitoring.

#### Saliva and ocular fluid

Among those accessible biological fluids, saliva is relatively easy to collect and it contains lots of meaningful biological information about health, such as metabolites, enzymes, hormones, proteins, microorganisms and ions.<sup>176</sup> However, because of the complexity of oral environment, the real-time continuous on-site detecting biomarkers in saliva is challenging. Higher requirements are demanded from in-mouth operation for biocompatibility of the sensors, besides that, the moist condition in the oral cavity and the large movement of mouth caused by chewing and talking bring difficulties to the integration of biosensors into mouth. In consequence, the saliva-based sensors to date are usually integrated with teeth or mouthguard.<sup>177–179</sup> To achieve this, Mannoer et al.<sup>177</sup> printed chemically modified graphene onto water-soluble silk. Via silk bioresorption, the graphene nanosensors can be transferred onto tooth enamel to detect pathogenic bacteria in saliva. Moreover, the resonant coil integrated in the nanosensor obviates onboard power and external connections. Kim et al.<sup>178,179</sup> developed mouthguard-based biosensors, which realized monitoring of salivary lactate and uric acid level. Although some studies indicate the good correlation between glucose in saliva and blood glucose, the composition of saliva is easily altered by the food or drink contamination, which restricts its applications in diabetes.<sup>180</sup> Because of close tear-blood concentration

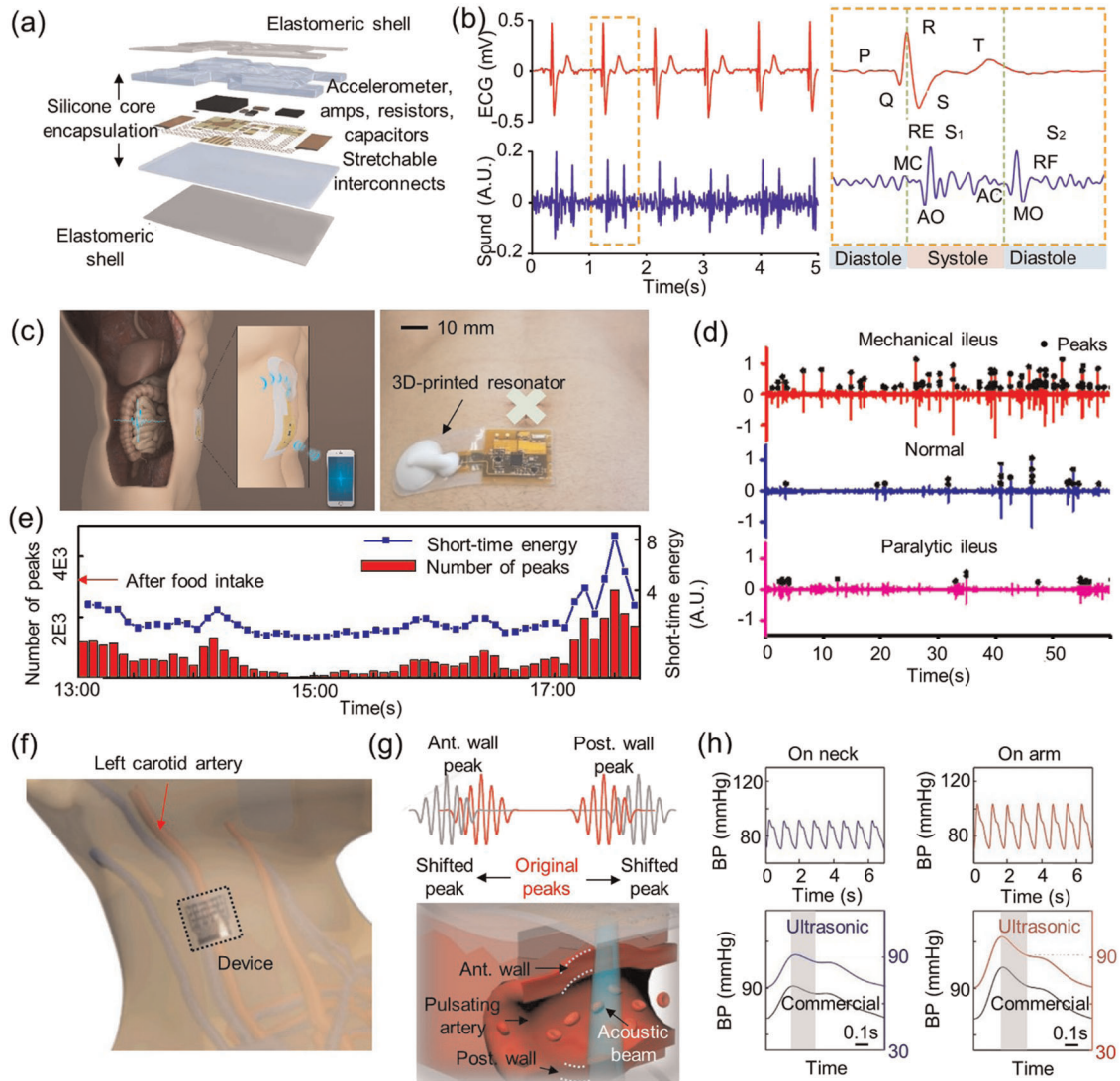


**Fig. 9 Flexible acoustic sensors and ultrasound devices.** **a** Exploded view diagram of a flexible acoustic sensor for detecting heart sound. **b** Heart sounds (bottom) and ECG (top) signals measured simultaneously and their magnified views. A.U. arbitrary units, MC mitral valve closure, AO aortic valve opening, RE rapid ventricular ejection, AC aortic valve closure, MO mitral valve opening, RF rapid ventricular filling. **c** Schematic (left) and photograph (right) of the flexible wearable wireless device for bowel sound detection. **d** Waveform lines of detected bowel sounds from one normal subject (blue line) and two patients with mechanical ileus (red line) and paralytic ileus (pink line). **e** Long time monitoring results of bowel sounds after meal. The red histogram shows the variation of number of peaks and the red broken line indicates the short-time energy of bowel sounds over time. **f** A stretchable ultrasonic device for monitoring of the central blood pressure. **g** Schematic illustration to measuring blood pressure by using pulse-echo method. Ant. anterior, Post. posterior. **h** Blood pressure measurements from carotid artery and brachial artery, and validation with a commercial tonometer.<sup>172</sup> (Copyright 2016, the American Association for the Advancement of Science). **c–e** Reproduced with permission<sup>174</sup> (Copyright 2019 Science China Press and Springer-Verlag GmbH Germany). **f–h** Reproduced with permission<sup>175</sup> (Copyright 2018, Nature Publish Group).

correlations, tear is an attractive biological fluid for its potential applications in non-invasive and continuous glucose monitoring, but is hard to access. Contact lenses provide a unique wearable platform for sensor and circuit integration as they realize continuous contact with tear fluids, at the same time without eye irritation and avoiding discomfort to the wearer.<sup>176</sup> The addition of complete electronic functional components (including sensor, antenna, interconnects and so on) within such small area of contact lenses platform may impact the field of vision of the subject. To ensure optical transparency for unobstructed vision and at the same time guarantee reliable mechanical and electrical properties, Kim et al.<sup>181</sup> introduced the graphene-silver nanowire hybrid electrode instead of opaque electronic materials, which provided the contact lenses sensor sufficient transparency (>91%) and stretchability (~25%).

### Sweat

Sweat is the most available biological fluid in human which is distributed over most of the body and can be accessed continuously.<sup>182</sup> The chemical components in it contain abundant valuable information about a person's health status, including metabolites (e.g., glucose, lactate, and alcohol) and electrolytes (e.g., potassium, calcium, and heavy metal ions).<sup>57</sup> It has been exploited for diagnosing diseases, such as diabetes, Cystic Fibrosis and diseases caused by abnormal concentration of heavy metals.<sup>183,184</sup>

As shown in Fig. 10a, the general structure of flexible electrochemical sensors consists of three components i.e., sweat-uptake layer, chemically modified sensor electrodes and encapsulation. Sweat-uptake layer contacts with the skin, absorbing and

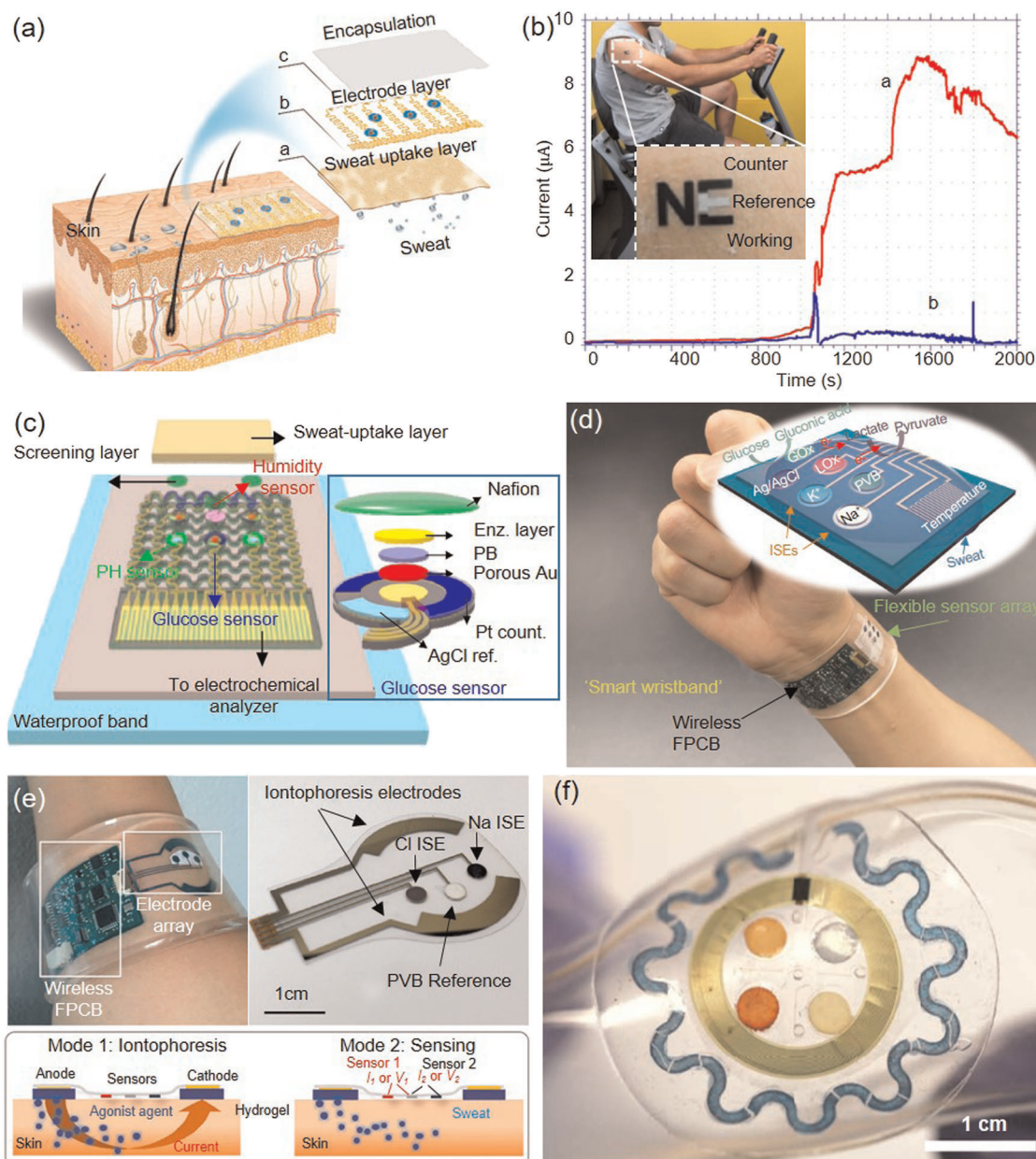


**Fig. 10** Flexible electrochemical sensors for non-invasive sweat analysis. **a** Common structure of flexible electrochemical sensors. **b** The tattoo biosensor used for monitoring of lactate in sweat. The graph shows the response of the lactate tattoo biosensors during the exercise. The insets exhibit the sensor attached to the skin and the three-electrode "NE" tattoo biosensor. **c** Schematic of the wearable sweat monitoring patch and the structure of the glucose sensor. **d** Fully integrated wearable sensor arrays for monitoring chemical elements in sweat. **e** The system of sweat extraction and sensing platform and relevant electrodes (top) and schematic illustrations of the iontophoresis and sensing modes (bottom). **f** The microfluidic device for the capture, storage, and colorimetric sensing of sweat. **b** Reproduced with permission<sup>65</sup> (Copyright 2013, American Chemical Society). **c** Reproduced with permission<sup>57</sup> (Copyright 2017, the American Association for the Advancement of Science). **d** Reproduced with permission<sup>59</sup> (Copyright 2016, Nature Publish Group). **e** Reproduced with permission<sup>188</sup> (Copyright 2017, National Academy of Sciences). **f** Reproduced with permission<sup>184</sup> (Copyright 2016, American Association for the Advancement of Science).

retaining sweat by capillary forces. Various of micro-porous materials have been explored as the sweat-uptake layer in the epidermal sweat sensors, such as recycled cellulose sponge, polyurethane sponge, polyvinyl alcohol sponge, cellulose paper and silicone sponge for epidermal analysis of sweat.<sup>185</sup> Chemically modified sensor electrodes convert the biochemical signals to electric ones, and the surface nanocrystallization could increase sensitivity.<sup>57</sup> Encapsulation envelops the sensor and provides soft support for wearing comfort.

Inspired by the conventional temporary tattoos, the first example of tattoo-based electrochemical electronics is fabricated via screen printing, which has enabled continuous chemical sensing by intimate contact with the skin.<sup>63</sup> Based on this technology, an epidermal electrochemical biosensor has been developed for real-time analysis of sweat lactate during exercise as shown in Fig. 10b.<sup>65</sup> The lactate sensor demonstrated high specificity toward sweat lactate and good resiliency against different deformation from physical activity. Later, this fabrication

methodology has been developed for diverse applications, such as monitoring sodium,<sup>66</sup> PH,<sup>68</sup> Alcohol,<sup>64</sup> and Glucose<sup>67</sup> in sweat.

As shown in Fig. 10c, recent progress has shown that the epidermal sweat-based glucose sensing and transdermal drug delivery can be integrated on a wearable patch.<sup>57</sup> The sweat collection and measuring accuracy are benefited by the integration of PH, temperature and humidity sensor as well as the miniaturization of the glucose sensor. To improve the electrochemical activity of sensors, porous gold electrode is formed by electrodeposition maximizing the electrochemically active surface area and strengthening the enzyme immobilization. A graphene-hybrid structure based electrode consists of the gold-doped graphene with a gold mesh is developed to enlarge the electrochemically active surface area while maintaining the flexibility and high conductivity of the device.<sup>56</sup>

To monitor multiple chemical components in sweat simultaneously, a series of fully integrated wearable sensors for sweat analysis have been developed, and the typical one is shown in Fig. 10d.<sup>59,186–188</sup> In these sensor arrays, different chemically modified electrodes for selectively monitoring calcium, sodium, potassium, heavy metal, lactates and glucose concentrations in sweat are fabricated on the flexible polyethylene terephthalate (PET) substrate by physical evaporation and electrochemical deposition methods. The sensing component is connected to a flexible printed circuit board for critical signal conditioning, processing, and wireless transmission. What's more, in order to exclude the influence caused by PH or temperature variation, the integrated system also integrated temperature sensor and PH sensor to compensate the sensors' readings. Thus, these fully integrated systems enable wearable, simultaneous, continuous and non-invasive sweat monitoring, which is of potential to enhance the conventional accurate analysis of chemical elements in human body that relies on bulky and expensive instruments.

Although rapid progress has been made in sweat-based sensor, it is still faced with many challenges, such as the comfortable and accurate measurement in the circumstance of less sweat (e.g., in cold climate or for the sedentary individuals) and the collection and storage of sweat. To solve the former question, actively stimulating sweat gland to secrete more sweat provides a solution. To extract enough sweat on-demand at certain locations, iontophoresis is a widely used method.<sup>64,188</sup> As shown in Fig. 10e, an electrochemically enhanced iontophoresis interface is integrated in the sensing system with various secretion profiles.<sup>188</sup> Results show that this device is of value in cystic diagnosis and the correlation studies of blood and sweat glucose. On the other hand, in order to realize wireless and power free monitoring and analysis of sweat, devices based on microfluidic systems have been reported, consisting of a network of functionalized channels and reservoirs where chemical analyses respond in colorimetric fashion is embedded as shown in Fig. 10f.<sup>184</sup> The sweat is captured and routed to the micro-channels and spatially separated regions for multi-parametric sensing of markers of interest.<sup>189–197</sup>

## Glucose

The wide spread diabetes and their need for long-term and accurate glycemic control make the glucose monitoring technologies, especially the non-invasive ones, most desirable and attractive, thus various schemes have been investigated, including optical and electrochemical ones.<sup>198</sup> Among them, wearable electrochemical glucose biosensors are most concerned. Many body fluids containing glucose can be deployed as the measuring target, such as sweat, skin ISF, tear and saliva, and so on. Sweat and skin ISF are the most commonly used samples in non-invasive glucose monitoring, and lots of devices have been developed.<sup>199,200</sup> ISF surrounds the tissue cells allowing the continuous exchange of small molecules between cells and capillaries, so it has the very similar composition of a number of clinically

important biomarkers to blood, such as protein, glucose, and ethanol contents. Especially, the concentration of glucose in ISF is one order larger than that in sweat.<sup>201</sup> Moreover, research using a subcutaneous glucose sensor shows that there is a just small time difference (about 4–10 min) between blood glucose and interstitial glucose.<sup>202</sup> Thus, the ISF is a good alternative to blood for glucose monitoring.

However, due to the barrier of skin, ISF couldn't be detected directly on the surface of skin. To achieve non-invasive continuous monitoring of glucose in ISF, reverse iontophoresis provides a solution. The process involves driving the uncharged and charged species from ISF passing through the dermis to the surface of skin with the application of a low electric current. In this way, detecting process can be non-invasive.<sup>203–205</sup> Tattoo-based device is an effective platform, as illustrated and photographed in Fig. 11a, b.<sup>67</sup> The results have shown that with this platform, reverse iontophoretic process, illustrated in Fig. 11c in time frame, dose help the extraction of ISF glucose and improve the current response for noninvasive glucose detection.<sup>67</sup>

Although reverse iontophoresis is a promising way to improve the efficiency of glucose measurement, there are still problems that need to be taken into further consideration, like the use of a high-density current and a long warm-up time may cause skin irritation. To ensure the enough amount of glucose driven out from the ISF in low-current occasions, Chen et al. have proposed a creative method of electrochemical twin channels (ETCs), which is schematically pictured in Fig. 11d.<sup>58,206</sup> With the help of an electric field, the hyaluronic acid is penetrated into the ISF changing the osmotic pressure in it, thus prompting intravascular blood glucose to be driven out of the vessel and transported to the skin surface. The flexible biocompatible paper battery and the ultrathin skin-like biosensors are integrated in the device, as shown in Fig. 11e.<sup>58</sup> Clinical trials demonstrate that the response of the biosensor with ETC is much higher and has a high correlation (>0.9) with clinically measured blood glucose levels, as shown in Fig. 11f.<sup>58</sup>

To truly implement the function of accurate glycermic control, the feedback therapy actions to the abnormal glucose level are indispensable, thus forming the close loop of the diabetes management. Microneedles and microneedle arrays have attracted a lot of interest recent years for their potentials in offering minimally invasive methods for bio-sensing and therapies through transcutaneous drug delivery by direct contact and interact with ISF. Transcutaneous microneedle patches have been reported as drug delivery system to be used in treatment of various diseases, such as diabetes and cancer.<sup>207–209</sup> Generally patches are based on a series of bio-responsive materials for controlled drug release by embedding drug-loaded micro-particles coated with bio-responsive material into microneedles, and the microneedles release the drug by responding to the biological conditions as demonstrated in Fig. 11g.<sup>210,211</sup> The therapy microneedles in electrochemical device consist of bioresorbable thermos-responsive materials, as shown in Fig. 11h.<sup>56</sup> When the glucose sensor detected over-threshold recordings the embedded heater shall be triggered to work, resulting in dissolving of outer phase change material and releasing of the drug in the microneedles.<sup>56,57</sup>

## DISCUSSION

After decades of development, the flexible inorganic bioelectronics have opened up many interdisciplinary research fields and expanded and enriched them rapidly with ever increasing speed. Biomedicine, which is expected to solve the issue of human health, is regarded as the most concerned application direction for flexible and stretchable bioelectronics both scientifically and commercially. Although lots of worldwide scientific works have offered abundant and striking results in materials, mechanics, designs and initial application in biomedicine of flexible and stretchable electronics, there is still plenty of room to be explored and constructed under

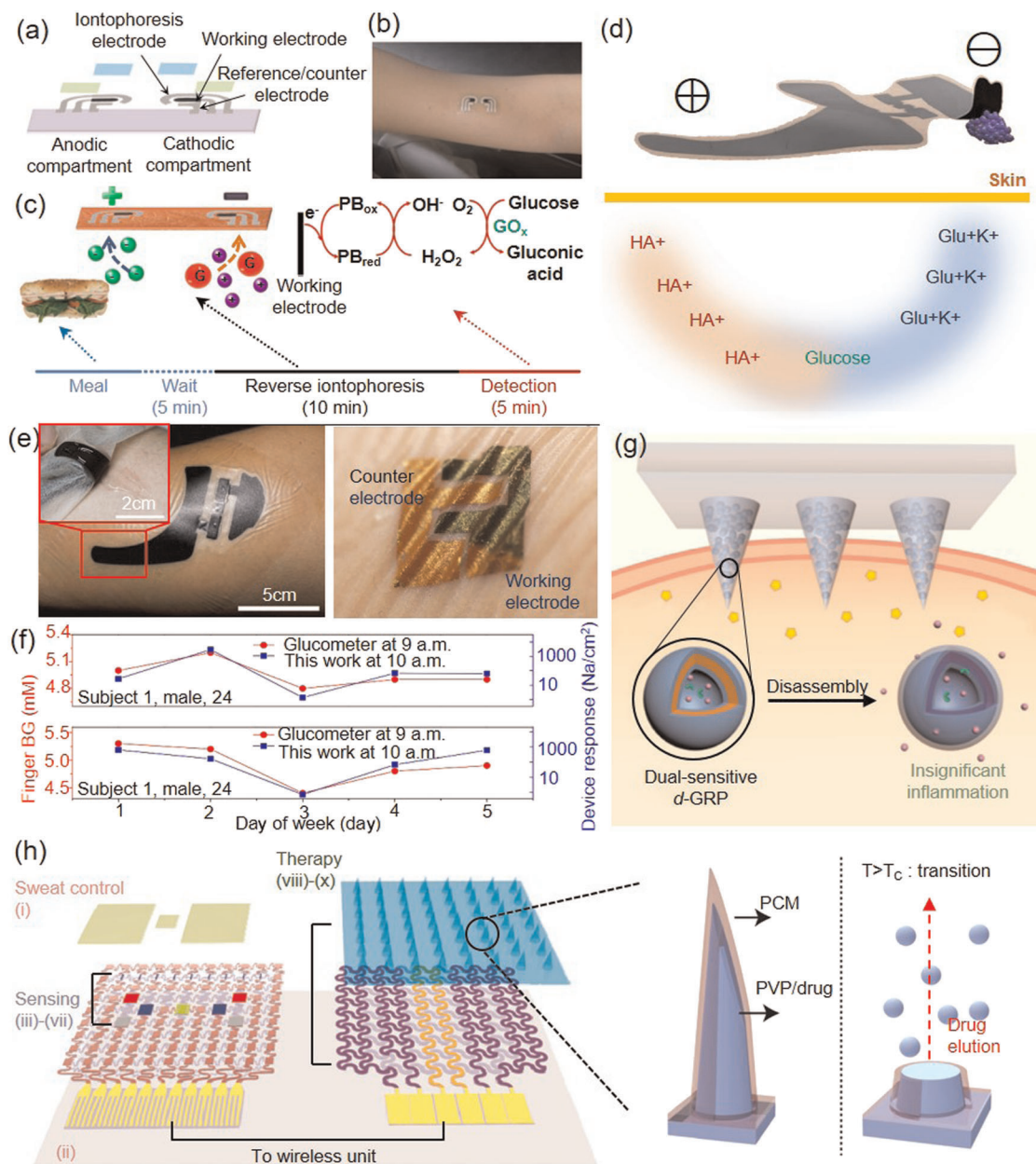


**Fig. 11 Non-invasive monitoring of glucose in interstitial fluid and the drug deliver by microneedles.** **a** Schematic of a tattoo-based glucose detection system that combines sensing module with the system for reverse iontophoresis. **b** Photograph of a tattoo-based glucose sensor applied to a human subject. **c** Schematic of the processes involved in monitoring glucose by tattoo-based glucose sensor with reverse iontophoresis. **d** Schematic of the ETCs, which perform HA penetration, glucose refiltration, and glucose outward transportation. **e** The flexible biocompatible paper battery (left) and the ultrathin skin-like biosensors (right) attached to the skin used for ETC measurement. The inset shows the hyaluronic acid sprayed under the paper battery anode. **f** Results of 5-day glucose monitoring with the glucometer (red) and ETC devices (blue). **g** Schematic of microneedle-array patch for in vivo insulin delivery triggered by a hyperglycemic state. **h** Schematic drawings of the diabetes patch, which is composed of the sweat-control (i, ii), sensing (iii)-(vii) and therapy (viii-x) components (left) and the drug-loaded disposable microneedles (right). **a-c** Reproduced with permission<sup>67</sup> (Copyright 2014, American Chemical Society). **e, f** Reproduced with permission<sup>58</sup> (Copyright 2017, American Association for the Advancement of Science). **g** Reproduced with permission<sup>211</sup> (Copyright 2017, American Chemical Society). **h** Reproduced with permission<sup>56</sup> (Copyright 2016, Nature Publish Group).

this topic. Here we provide our views from the perspective of scientific research as well as the industrialization.

For the aspect of scientific research, the potential research directions of interests are the following yet not limited to, (1) to further improve the integrated level of the devices, such as integrating multi-function in a single device by multi-layer structure design or minimizing each functional unit; (2) to develop closed-loop systems that contain real-time monitoring

and therapy unit; (3) to develop energy solutions that are as flexible, stretchable and biocompatible as the well-developed sensors and circuits; (4) to explore new biomedical applications where the bio-environment much more complicated than human skin, like inside the human heart, brain tissue or pulmonary alveolus; (5) to investigate in the science problems that lie on the way of scientific research to industrialization, such as the stability, fatigue, and robust issue of the devices, to offer

the solutions with new materials, structure designs or systematic mechanisms.

From the perspective of industrialization, the blanks concentrate mainly on the mass production technology as well as the standards which are used to evaluate and assess the springing-up products.<sup>212</sup> The mass production technology includes both fabrication equipment and testing machines, since the current technology cannot be directly used to product flexible and stretchable electronics, especially for biomedical devices. The initial trial has been conducted in Europe in manufacturing transfer printing machine. Besides, when more and more products had been brought out, professional standards would be needed to evaluate their properties, like stretchability, flexibility, biocompatibility and so on, thus paving the rules and regulations for the process of industrialization. Hopefully, with the joint endeavor in science and industry, the day when we enjoy all kinds of flexible and stretchable biomedical devices improved living life would come soon.

## DATA AVAILABILITY

All data are available within the article or available from the authors upon reasonable request.

Received: 14 June 2019; Accepted: 12 December 2019;

Published online: 04 February 2020

## REFERENCES

- Rogers, J., Malliaras, G. & Someya, T. Biomedical devices go wild. *Sci. Adv.* **4**, eaav1889 (2018).
- Choi, S., Lee, H., Ghaffari, R., Hyeon, T. & Kim, D. H. Recent advances in flexible and stretchable bio-electronic devices integrated with nanomaterials. *Adv. Mater.* **28**, 4203–4218 (2016).
- Ray, T. R. et al. Bio-integrated wearable systems: a comprehensive review. *Chem. Rev.* **119**, 5461–5533 (2019).
- Miyamoto, A. et al. Inflammation-free, gas-permeable, lightweight, stretchable on-skin electronics with nanomeshes. *Nat. Nanotechnol.* **12**, 907 (2017).
- Chou, H.-H. et al. A chameleon-inspired stretchable electronic skin with interactive colour changing controlled by tactile sensing. *Nat. Commun.* **6**, 8011 (2015).
- Trung, T. Q., Ramasundaram, S., Hwang, B. U. & Lee, N. E. An all-elastomeric transparent and stretchable temperature sensor for body-attachable wearable electronics. *Adv. Mater.* **28**, 502–509 (2016).
- Zhao, H., O'Brien, K., Li, S. & Shepherd, R. F. Optoelectronically innervated soft prosthetic hand via stretchable optical waveguides. *Sci. Robot.* **1**, eaai7529 (2016).
- Ho, D. H. et al. Stretchable and multimodal all graphene electronic skin. *Adv. Mater.* **28**, 2601–2608 (2016).
- Trung, T. Q. & Lee, N. E. Recent progress on stretchable electronic devices with intrinsically stretchable components. *Adv. Mater.* **29**, 1603167 (2017).
- Trung, T. Q. & Lee, N. E. Flexible and stretchable physical sensor integrated platforms for wearable human-activity monitoring and personal healthcare. *Adv. Mater.* **28**, 4338–4372 (2016).
- Dickey, M. D. Stretchable and soft electronics using liquid metals. *Adv. Mater.* **29**, 1606425 (2017).
- Yao, S. & Zhu, Y. Nanomaterial-enabled stretchable conductors: strategies, materials and devices. *Adv. Mater.* **27**, 1480–1511 (2015).
- Liu, W., Song, M. S., Kong, B. & Cui, Y. Flexible and stretchable energy storage: recent advances and future perspectives. *Adv. Mater.* **29**, 1603436 (2017).
- Larson, C. et al. Highly stretchable electroluminescent skin for optical signaling and tactile sensing. *Science* **351**, 1071–1074 (2016).
- Oh, J. Y. et al. Intrinsically stretchable and healable semiconducting polymer for organic transistors. *Nature* **539**, 411 (2016).
- Bao, Z. & Chen, X. Flexible and stretchable devices. *Adv. Mater.* **28**, 4177–4179 (2016).
- Wang, Y. et al. A highly stretchable, transparent, and conductive polymer. *Sci. Adv.* **3**, e1602076 (2017).
- Lee, W. et al. Transparent, conformable, active multielectrode array using organic electrochemical transistors. *Proc. Natl Acad. Sci. USA* **114**, 10554–10559 (2017).
- Someya, T., Bao, Z. & Malliaras, G. G. The rise of plastic bioelectronics. *Nature* **540**, 379–385 (2016).
- Lipomi, D. J. & Bao, Z. Stretchable and ultraflexible organic electronics. *MRS Bull.* **42**, 93–97 (2017).
- Xu, J. et al. Highly stretchable polymer semiconductor films through the nanoconfinement effect. *Science* **355**, 59–64 (2017).
- Yan, X. et al. Quadruple H-bonding cross-linked supramolecular polymeric materials as substrates for stretchable, antitearing, and self-healable thin film electrodes. *J. Am. Chem. Soc.* **140**, 5280–5289 (2018).
- Rogers, J. A., Someya, T. & Huang, Y. Materials and mechanics for stretchable electronics. *Science* **327**, 1603–1607 (2010).
- Khang, D.-Y., Jiang, H., Huang, Y. & Rogers, J. A. A stretchable form of single-crystal silicon for high-performance electronics on rubber substrates. *Science* **311**, 208–212 (2006).
- Cao, Y. et al. Direct fabrication of stretchable electronics on a polymer substrate with process-integrated programmable rigidity. *Adv. Funct. Mater.* **28**, 1804604 (2018).
- Li, H. et al. Epidermal inorganic optoelectronics for blood oxygen measurement. *Adv. Healthc. Mater.* **6**, 1601013 (2017).
- Han, Z. et al. Fabrication of highly pressure-sensitive, hydrophobic, and flexible 3D carbon nanofiber networks by electrospinning for human physiological signal monitoring. *Nanoscale* **11**, 5942–5950 (2019).
- Ma, Y. et al. Relation between blood pressure and pulse wave velocity for human arteries. *Proc. Natl Acad. Sci. USA* **115**, 11144–11149 (2018).
- Han, S. et al. Battery-free, wireless sensors for full-body pressure and temperature mapping. *Sci. Transl. Med.* **10**, eaan4950 (2018).
- Liu, Z. et al. High-adhesion stretchable electrodes based on nanopile interlocking. *Adv. Mater.* **29**, 1603382 (2017).
- Su, Y. et al. Elasticity of fractal inspired interconnects. *Small* **11**, 367–373 (2015).
- Ma, Q. & Zhang, Y. Mechanics of fractal-inspired horseshoe microstructures for applications in stretchable electronics. *J. Appl. Mech.* **83**, 111008 (2016).
- Zhang, Y. et al. Mechanics of ultra-stretchable self-similar serpentine interconnects. *Acta Materialia* **61**, 7816–7827 (2013).
- Fu, H. et al. Lateral buckling and mechanical stretchability of fractal interconnects partially bonded onto an elastomeric substrate. *Appl. Phys. Lett.* **106**, 091902 (2015).
- Zhang, Y. et al. A hierarchical computational model for stretchable interconnects with fractal-inspired designs. *J. Mech. Phys. Solids* **72**, 115–130 (2014).
- Zhang, Y., Huang, Y. & Rogers, J. A. Mechanics of stretchable batteries and supercapacitors. *Curr. Opin. Solid State Mater. Sci.* **19**, 190–199 (2015).
- Zhang, Y. et al. Experimental and theoretical studies of serpentine microstructures bonded to prestrained elastomers for stretchable electronics. *Adv. Funct. Mater.* **24**, 2028–2037 (2014).
- Lü, C. et al. Mechanics of tunable hemispherical electronic eye camera systems that combine rigid device elements with soft elastomers. *J. Appl. Mech.* **80**, 061022 (2013).
- Su, Y. et al. Mechanics of stretchable electronics on balloon catheter under extreme deformation. *Int. J. Solids Struct.* **51**, 1555–1561 (2014).
- Shi, X. et al. Mechanics design for stretchable, high areal coverage GaAs solar module on an ultrathin substrate. *J. Appl. Mech.* **81**, 124502 (2014).
- Gao, L. et al. Optics and nonlinear buckling mechanics in large-area, highly stretchable arrays of plasmonic nanostructures. *ACS Nano* **9**, 5968–5975 (2015).
- Ma, Q. et al. A nonlinear mechanics model of bio-inspired hierarchical lattice materials consisting of horseshoe microstructures. *J. Mech. Phys. Solids* **90**, 179–202 (2016).
- Yuan, J. et al. A Mechanics model for sensors imperfectly bonded to the skin for determination of the young's moduli of epidermis and dermis. *J. Appl. Mech.* **83**, 084501 (2016).
- Su, Y. et al. In-plane deformation mechanics for highly stretchable electronics. *Adv. Mater.* **29**, 1604989 (2017).
- Carlson, A., Bowen, A. M., Huang, Y., Nuzzo, R. G. & Rogers, J. A. Transfer printing techniques for materials assembly and micro/nanodevice fabrication. *Adv. Mater.* **24**, 5284–5318 (2012).
- Cheng, H. et al. An analytical model for shear-enhanced adhesiveless transfer printing. *Mech. Res. Commun.* **43**, 46–49 (2012).
- Yang, S. Y. et al. Elastomer surfaces with directionally dependent adhesion strength and their use in transfer printing with continuous roll-to-roll applications. *Adv. Mater.* **24**, 2117–2122 (2012).
- Meitl, M. A. et al. Transfer printing by kinetic control of adhesion to an elastomeric stamp. *Nat. Mater.* **5**, 33–38 (2006).
- Feng, X. et al. Competing fracture in kinetically controlled transfer printing. *Langmuir* **23**, 12555–12560 (2007).
- Chen, H., Feng, X., Huang, Y., Huang, Y. & Rogers, J. A. Experiments and viscoelastic analysis of peel test with patterned strips for applications to transfer printing. *J. Mech. Phys. Solids* **61**, 1737–1752 (2013).

51. Chen, H., Feng, X. & Chen, Y. Directionally controlled transfer printing using micropatterned stamps. *Appl. Phys. Lett.* **103**, 151607 (2013).
52. Cheng, H. et al. A viscoelastic model for the rate effect in transfer printing. *J. Appl. Mech.* **80**, 041019 (2013).
53. Huang, Y. et al. Direct laser writing-based programmable transfer printing via bioinspired shape memory reversible adhesive. *ACS Appl. Mater. Interfaces* **8**, 35628–35633 (2016).
54. Eisenhaure, J. D. et al. The use of shape memory polymers for microassembly by transfer printing. *J. Microelectromechanical Syst.* **23**, 1012–1014 (2014).
55. Kim, D.-H. et al. Dissolvable films of silk fibroin for ultrathin conformal bio-integrated electronics. *Nat. Mater.* **9**, 511 (2010).
56. Lee, H. et al. A graphene-based electrochemical device with thermoresponsive microneedles for diabetes monitoring and therapy. *Nat. Nanotechnol.* **11**, 566 (2016).
57. Lee, H. et al. Wearable/disposable sweat-based glucose monitoring device with multistage transdermal drug delivery module. *Sci. Adv.* **3**, e1601314 (2017).
58. Chen, Y. et al. Skin-like biosensor system via electrochemical channels for noninvasive blood glucose monitoring. *Sci. Adv.* **3**, e1701629 (2017).
59. Gao, W. et al. Fully integrated wearable sensor arrays for multiplexed in situ perspiration analysis. *Nature* **529**, 509 (2016).
60. Kim, J. et al. Miniaturized battery-free wireless systems for wearable pulse oximetry. *Adv. Funct. Mater.* **27**, 1604373 (2017).
61. Sezen, M., Register, J. T., Yao, Y., Glisic, B. & Loo, Y. L. Eliminating piezoresistivity in flexible conducting polymers for accurate temperature sensing under dynamic mechanical deformations. *Small* **12**, 2832–2838 (2016).
62. Sinex, J. E. Pulse oximetry: principles and limitations. *Am. J. Emerg. Med.* **17**, 59–66 (1999).
63. Windmiller, J. R. et al. Electrochemical sensing based on printable temporary transfer tattoos. *Chem. Commun.* **48**, 6794–6796 (2012).
64. Kim, J. et al. Noninvasive alcohol monitoring using a wearable tattoo-based iontophoretic-biosensing system. *ACS Sens.* **1**, 1011–1019 (2016).
65. Jia, W. et al. Electrochemical tattoo biosensors for real-time noninvasive lactate monitoring in human perspiration. *Anal. Chem.* **85**, 6553–6560 (2013).
66. Bandodkar, A. J. et al. Epidermal tattoo potentiometric sodium sensors with wireless signal transduction for continuous non-invasive sweat monitoring. *Biosens. Bioelectron.* **54**, 603–609 (2014).
67. Bandodkar, A. J. et al. Tattoo-based noninvasive glucose monitoring: a proof-of-concept study. *Anal. Chem.* **87**, 394–398 (2014).
68. Bandodkar, A. J. et al. Tattoo-based potentiometric ion-selective sensors for epidermal pH monitoring. *Analyst* **138**, 123–128 (2013).
69. Xue, Z., Song, H., Rogers, J. A., Zhang, Y. & Huang, Y. Mechanically-guided structural designs in stretchable inorganic electronics. *Adv. Mater.* **31**, 1902254 (2019).
70. Park, Y. J., Lee, S.-K., Kim, M.-S., Kim, H. & Ahn, J.-H. Graphene-based conformal devices. *ACS Nano* **8**, 7655–7662 (2014).
71. Park, Y. et al. Microtopography-guided conductive patterns of liquid-driven graphene nanoplatelet networks for stretchable and skin-conformal sensor array. *Adv. Mater.* **29**, 1606453 (2017).
72. Changhyun, P. et al. Highly skin-conformal microhair sensor for pulse signal amplification. *Adv. Mater.* **27**, 634–640 (2015).
73. Ma, Y. et al. Design of strain-limiting substrate materials for stretchable and flexible electronics. *Adv. Funct. Mater.* **26**, 5345–5351 (2016).
74. Ma, Y., Feng, X., Rogers, J. A., Huang, Y. & Zhang, Y. Design and application of 'J-shaped' stress-strain behavior in stretchable electronics: a review. *Lab a Chip* **17**, 1689–1704 (2017).
75. Jang, K.-I. et al. Soft network composite materials with deterministic and bio-inspired designs. *Nat. Commun.* **6**, 6566 (2015).
76. Yang, W. et al. A breathable and screen-printed pressure sensor based on nanofiber membranes for electronic skins. *Adv. Mater. Technol.* **3**, 1700241 (2018).
77. Haddad, P., Servati, A., Soltanian, S., Ko, F. & Servati, P. Breathable dry silver/silver chloride electronic textile electrodes for electrodermal activity monitoring. *Biosensors* **8**, 79 (2018).
78. Gong, M. et al. Flexible breathable nanomesh electronic devices for on-demand therapy. *Adv. Funct. Mater.* **29**, 1902127 (2019).
79. Fan, Y. J. et al. Highly robust, transparent, and breathable epidermal electrode. *ACS Nano* **12**, 9326–9332 (2018).
80. Chen, Y., Lu, B., Chen, Y. & Feng, X. Breathable and stretchable temperature sensors inspired by skin. *Sci. Rep.* **5**, 11505 (2015).
81. Yu, K. J. et al. Bioresorbable silicon electronics for transient spatiotemporal mapping of electrical activity from the cerebral cortex. *Nat. Mater.* **15**, 782 (2016).
82. Kang, S.-K., Koo, J., Lee, Y. K. & Rogers, J. A. Advanced materials and devices for bioresorbable electronics. *Acc. Chem. Res.* **51**, 988–998 (2018).
83. Xu, B. et al. An epidermal stimulation and sensing platform for sensorimotor prosthetic control, management of lower back exertion, and electrical muscle activation. *Adv. Mater.* **28**, 4462–4471 (2016).
84. Lin, S. et al. Stretchable hydrogel electronics and devices. *Adv. Mater.* **28**, 4497–4505 (2016).
85. Jeong, J. W. et al. Capacitive epidermal electronics for electrically safe, long-term electrophysiological measurements. *Adv. Healthc. Mater.* **3**, 642–648 (2014).
86. Chen, G. et al. Plasticizing silk protein for on-skin stretchable electrodes. *Adv. Mater.* **30**, 1800129 (2018).
87. Xiu, Z.-m., Zhang, Q.-b., Puppala, H. L., Colvin, V. L. & Alvarez, P. J. Negligible particle-specific antibacterial activity of silver nanoparticles. *Nano Lett.* **12**, 4271–4275 (2012).
88. Karthik, P. & Singh, S. P. Conductive silver inks and their applications in printed and flexible electronics. *Rsc Adv.* **5**, 77760–77790 (2015).
89. Chen, Y. et al. Highly flexible, transparent, conductive and antibacterial films made of spin-coated silver nanowires and a protective ZnO layer. *Phys. E: Low-Dimensional Syst. Nanostruct.* **76**, 88–94 (2016).
90. Zhang, Y.-F., Ren, Y.-J., Guo, H.-C. & Bai, S.-I. Enhanced thermal properties of PDMS composites containing vertically aligned graphene tubes. *Appl. Therm. Eng.* **150**, 840–848 (2019).
91. Yin, Y., Cui, Y., Li, Y., Xing, Y. & Li, M. Thermal management of flexible wearable electronic devices integrated with human skin considering clothing effect. *Appl. Therm. Eng.* **144**, 504–511 (2018).
92. Song, J., Chen, C. & Zhang, Y. High thermal conductivity and stretchability of layer-by-layer assembled silicone rubber/graphene nanosheets multilayered films. *Compos. Part A: Appl. Sci. Manuf.* **105**, 1–8 (2018).
93. Jung, H. H. et al. Thin metallic heat sink for interfacial thermal management in biointegrated optoelectronic devices. *Adv. Mater. Technol.* **3**, 1800159 (2018).
94. Hong, H. et al. Anisotropic thermal conductive composite by the guided assembly of boron nitride nanosheets for flexible and stretchable electronics. *Adv. Funct. Mater.* **29**, 1902575 (2019).
95. Chen, J., Huang, X., Sun, B. & Jiang, P. Highly thermally conductive yet electrically insulating polymer/boron nitride nanosheets nanocomposite films for improved thermal management capability. *ACS Nano* **13**, 337–345 (2018).
96. Niedermeyer, E. & da Silva, F. L. *Electroencephalography: Basic Principles, Clinical Applications, and Related Fields* (Lippincott Williams & Wilkins, 2005).
97. Deuschl, G. & Eisen, A. Recommendations for the practice of clinical neurophysiology: Guidelines of the International Federation of Clinical Neurophysiology (1999).
98. Kuzum, D. et al. Transparent and flexible low noise graphene electrodes for simultaneous electrophysiology and neuroimaging. *Nat. Commun.* **5**, 5259 (2014).
99. Yan, Z. et al. Thermal release transfer printing for stretchable conformal bioelectronics. *Adv. Sci.* **4**, 1700251 (2017).
100. Rubehn, B., Bosman, C., Oostenveld, R., Fries, P. & Stieglitz, T. A MEMS-based flexible multichannel ECoG-electrode array. *J. Neural Eng.* **6**, 036003 (2009).
101. Castagnola, E. et al. PEDOT-CNT-coated low-impedance, ultra-flexible, and brain-conformable micro-ECoG arrays. *IEEE Trans. Neural Syst. Rehabilitation Eng.* **23**, 342–350 (2015).
102. Park, D.-W. et al. Graphene-based carbon-layered electrode array technology for neural imaging and optogenetic applications. *Nat. Commun.* **5**, ncomms6258 (2014).
103. Blau, A. et al. Flexible, all-polymer microelectrode arrays for the capture of cardiac and neuronal signals. *Biomaterials* **32**, 1778–1786 (2011).
104. Toda, H. et al. Simultaneous recording of ECoG and intracortical neuronal activity using a flexible multichannel electrode-mesh in visual cortex. *Neuroimage* **54**, 203–212 (2011).
105. Viventi, J. et al. Flexible, foldable, actively multiplexed, high-density electrode array for mapping brain activity in vivo. *Nat. Neurosci.* **14**, 1599 (2011).
106. Kang, S.-K. et al. Bioresorbable silicon electronic sensors for the brain. *Nature* **530**, 71–76 (2016).
107. Navarro, X. et al. A critical review of interfaces with the peripheral nervous system for the control of neuroprostheses and hybrid bionic systems. *J. Peripheral Nerv. Syst.* **10**, 229–258 (2005).
108. Xiang, Z. et al. Progress of flexible electronics in neural interfacing – a self-adaptive non-invasive neural ribbon electrode for small nerves recording. *Adv. Mater.* **28**, 4472–4479 (2016).
109. Hassler, C., Boretius, T. & Stieglitz, T. Polymers for neural implants. *J. Polym. Sci. Part B: Polym. Phys.* **49**, 18–33 (2011).
110. Ma, Y. et al. Flexible hybrid electronics for digital healthcare. *Adv. Mater.* **0**, 1902062 (2019).
111. Grill, W. M., Norman, S. E. & Bellamkonda, R. V. Implanted neural interfaces: biochallenges and engineered solutions. *Annu. Rev. Biomed. Eng.* **11**, 1–24 (2009).

112. Zhang, Y. et al. Climbing-inspired twining electrodes using shape memory for peripheral nerve stimulation and recording. *Sci. Adv.* **5**, eaaw1066 (2019).
113. Xu, L. et al. 3D multifunctional integumentary membranes for spatiotemporal cardiac measurements and stimulation across the entire epicardium. *Nat. Commun.* **5**, ncomms4329 (2014).
114. Kim, D.-H. et al. Electronic sensor and actuator webs for large-area complex geometry cardiac mapping and therapy. *Proc. Natl Acad. Sci. USA* **109**, 19910–19915 (2012).
115. Xu, L. et al. Materials and fractal designs for 3D multifunctional integumentary membranes with capabilities in cardiac electrotherapy. *Adv. Mater.* **27**, 1731–1737 (2015).
116. Chung, H. J. et al. Stretchable, multiplexed pH sensors with demonstrations on rabbit and human hearts undergoing ischemia. *Adv. Healthc. Mater.* **3**, 59–68 (2014).
117. Kim, D. H. et al. Materials for multifunctional balloon catheters with capabilities in cardiac electrophysiological mapping and ablation therapy. *Nat. Mater.* **10**, 316–323 (2011).
118. Viventi, J. et al. A conformal, bio-interfaced class of silicon electronics for mapping cardiac electrophysiology. *Sci. Transl. Med.* **2**, 24ra22–24ra22 (2010).
119. Park, J. et al. Electromechanical cardioplasty using a wrapped elasto-conductive epicardial mesh. *Sci. Transl. Med.* **8**, 344ra86 (2016).
120. Choi, S. et al. Highly conductive, stretchable and biocompatible Ag–Au core–sheath nanowire composite for wearable and implantable bioelectronics. *Nat. Nanotechnol.* **13**, 1048–1056 (2018).
121. Xu, L. et al. 3D multifunctional integumentary membranes for spatiotemporal cardiac measurements and stimulation across the entire epicardium. *Nat. Commun.* **5**, 3329 (2014).
122. Jeong, J. W. et al. Materials and optimized designs for human-machine interfaces via epidermal electronics. *Adv. Mater.* **25**, 6839–6846 (2013).
123. Kim, S. J. et al. Stretchable and transparent biointerface using cell-sheet–graphene hybrid for electrophysiology and therapy of skeletal muscle. *Adv. Funct. Mater.* **26**, 3207–3217 (2016).
124. Bouton, C. E. et al. Restoring cortical control of functional movement in a human with quadriplegia. *Nature* **533**, 247 (2016).
125. Webb, R. C. et al. Ultrathin conformal devices for precise and continuous thermal characterization of human skin. *Nat. Mater.* **12**, 938 (2013).
126. Kim, D. H. et al. Thin, flexible sensors and actuators as ‘instrumented’ surgical sutures for targeted wound monitoring and therapy. *Small* **8**, 3263–3268 (2012).
127. Bendi, R. et al. Self-powered graphene thermistor. *Nano Energy* **26**, 586–594 (2016).
128. Chaoyi, Y., Jiangxin, W. & Pooi See, L. Stretchable graphene thermistor with tunable thermal index. *ACS Nano* **9**, 2130 (2015).
129. Shih, W.-P. et al. Flexible temperature sensor array based on a graphite-polydimethylsiloxane composite. *Sensors* **10**, 3597–3610 (2010).
130. Gao, L. et al. Epidermal photonic devices for quantitative imaging of temperature and thermal transport characteristics of the skin. *Nat. Commun.* **5**, 4938 (2014).
131. Stücker, M. et al. The cutaneous uptake of atmospheric oxygen contributes significantly to the oxygen supply of human dermis and epidermis. *J. Physiol.* **538**, 985–994 (2010).
132. Huang, Y., Chen, H., Wu, J. & Feng, X. Controllable wrinkle configurations by soft micro-patterns to enhance the stretchability of Si ribbons. *Soft Matter* **10**, 2559–2566 (2014).
133. Sheng, X. et al. Soft microfluidic assemblies of sensors, circuits, and radios for the skin. *Science* **344**, 70–74 (2014).
134. Webb, R. C. et al. Epidermal devices for noninvasive, precise, and continuous mapping of macrovascular and microvascular blood flow. *Sci. Adv.* **1**, e1500701 (2015).
135. Hattori, Y. et al. Multifunctional skin-like electronics for quantitative, clinical monitoring of cutaneous wound healing. *Adv. Healthc. Mater.* **3**, 1597–1607 (2014).
136. Amjadi, M., Kyung, K. U., Park, I. & Sitti, M. Stretchable, skin-mountable, and wearable strain sensors and their potential applications: a review. *Adv. Funct. Mater.* **26**, 1678–1698 (2016).
137. Nur, R. et al. A highly sensitive capacitive-type strain sensor using wrinkled ultrathin gold films. *Nano Lett.* **18**, 5610–5617 (2018).
138. Chen, Y., Lu, B., Chen, Y. & Feng, X. Biocompatible and ultra-flexible inorganic strain sensors attached to skin for long-term vital signs monitoring. *IEEE Electron Device Lett.* **37**, 496–499 (2016).
139. Nesser, H., Grisolia, J., Alnasser, T., Viallet, B. & Ressler, L. Towards wireless highly sensitive capacitive strain sensors based on gold colloidal nanoparticles. *Nanoscale* **10**, 10479–10487 (2018).
140. Kim, K. K. et al. Highly sensitive and stretchable multidimensional strain sensor with prestrained anisotropic metal nanowire percolation networks. *Nano Lett.* **15**, 5240–5247 (2015).
141. Ho, M. D. et al. Percolating network of ultrathin gold nanowires and silver nanowires toward “invisible” wearable sensors for detecting emotional expression and apexcardiogram. *Adv. Funct. Mater.* **27**, 1700845 (2017).
142. Lee, H., Seong, B., Moon, H. & Byun, D. Directly printed stretchable strain sensor based on ring and diamond shaped silver nanowire electrodes. *Rsc Adv.* **5**, 28379–28384 (2015).
143. Chossat, J.-B., Park, Y.-L., Wood, R. J. & Duchaine, V. A soft strain sensor based on ionic and metal liquids. *IEEE Sens. J.* **13**, 3405–3414 (2013).
144. Cooper, C. B. et al. Stretchable capacitive sensors of torsion, strain, and touch using double helix liquid metal fibers. *Adv. Funct. Mater.* **27**, 1605630 (2017).
145. Cai, L. et al. Super-stretchable, transparent carbon nanotube-based capacitive strain sensors for human motion detection. *Sci. Rep.* **3**, 3048 (2013).
146. Roh, E., Hwang, B.-U., Kim, D., Kim, B.-Y. & Lee, N.-E. Stretchable, transparent, ultrasensitive, and patchable strain sensor for human–machine interfaces comprising a nanohybrid of carbon nanotubes and conductive elastomers. *ACS Nano* **9**, 6252–6261 (2015).
147. Ryu, S. et al. Extremely elastic wearable carbon nanotube fiber strain sensor for monitoring of human motion. *ACS Nano* **9**, 5929–5936 (2015).
148. Shi, J. et al. Graphene reinforced carbon nanotube networks for wearable strain sensors. *Adv. Funct. Mater.* **26**, 2078–2084 (2016).
149. Zhou, J., Yu, H., Xu, X., Han, F. & Lubineau, G. Ultrasensitive, stretchable strain sensors based on fragmented carbon nanotube papers. *ACS Appl. Mater. Interfaces* **9**, 4835–4842 (2017).
150. Bae, S.-H. et al. Graphene-based transparent strain sensor. *Carbon* **51**, 236–242 (2013).
151. Qin, Y. et al. Lightweight, superelastic, and mechanically flexible graphene/polyimide nanocomposite foam for strain sensor application. *ACS Nano* **9**, 8933–8941 (2015).
152. Liu, Q., Chen, J., Li, Y. & Shi, G. High-performance strain sensors with fish-scale-like graphene-sensing layers for full-range detection of human motions. *ACS Nano* **10**, 7901–7906 (2016).
153. Chen, S., Wei, Y., Yuan, X., Lin, Y. & Liu, L. A highly stretchable strain sensor based on a graphene/silver nanoparticle synergic conductive network and a sandwich structure. *J. Mater. Chem. C* **4**, 4304–4311 (2016).
154. Lou, Z., Chen, S., Wang, L., Jiang, K. & Shen, G. An ultra-sensitive and rapid response speed graphene pressure sensors for electronic skin and health monitoring. *Nano Energy* **23**, 7–14 (2016).
155. Lu, N., Lu, C., Yang, S. & Rogers, J. Highly sensitive skin-mountable strain gauges based entirely on elastomers. *Adv. Funct. Mater.* **22**, 4044–4050 (2012).
156. Wu, X., Han, Y., Zhang, X., Zhou, Z. & Lu, C. Large-area compliant, low-cost, and versatile pressure-sensing platform based on microcrack-designed carbon black/polyurethane sponge for human–machine interfacing. *Adv. Funct. Mater.* **26**, 6246–6256 (2016).
157. Yamada, T. et al. A stretchable carbon nanotube strain sensor for human-motion detection. *Nat. Nanotechnol.* **6**, 296 (2011).
158. Dagdeviren, C. et al. Conformable amplified lead zirconate titanate sensors with enhanced piezoelectric response for cutaneous pressure monitoring. *Nat. Commun.* **5**, 4496 (2014).
159. Miller, S. & Bao, Z. Fabrication of flexible pressure sensors with microstructured polydimethylsiloxane dielectrics using the breath figures method. *J. Mater. Res.* **30**, 3584–3594 (2015).
160. Tee, B. C. K. et al. Tunable flexible pressure sensors using microstructured elastomer geometries for intuitive electronics. *Adv. Funct. Mater.* **24**, 5427–5434 (2015).
161. Park, S. et al. Stretchable energy harvesting tactile electronic skin capable of differentiating multiple mechanical stimuli modes. *Adv. Mater.* **26**, 7324–7332 (2014).
162. Boutry, C. M. et al. A hierarchically patterned, bioinspired e-skin able to detect the direction of applied pressure for robotics. *Sci. Robot.* **3**, eaau6914 (2018).
163. Jian, M. et al. Flexible and highly sensitive pressure sensors based on bionic hierarchical structures. *Adv. Funct. Mater.* **27**, 1606066 (2017).
164. Park, J., Kim, M., Lee, Y., Lee, H. S. & Ko, H. Fingertip skin-inspired microstructured ferroelectric skins discriminate static/dynamic pressure and temperature stimuli. *Sci. Adv.* **1**, e1500661 (2015).
165. Park, J. et al. Giant tunneling piezoresistance of composite elastomers with interlocked microdome arrays for ultrasensitive and multimodal electronic skins. *ACS Nano* **8**, 4689–4697 (2014).
166. Shao, Q. et al. High-performance and tailorable pressure sensor based on ultrathin conductive polymer film. *Small* **10**, 1466–1472 (2014).
167. Zhu, B. et al. Microstructured graphene arrays for highly sensitive flexible tactile sensors. *Small* **10**, 3625–3631 (2014).
168. Han, J.-W., Kim, B., Li, J. & Meyyappan, M. Flexible, compressible, hydrophobic, floatable, and conductive carbon nanotube-polymer sponge. *Appl. Phys. Lett.* **102**, 051903 (2013).

169. Zhuo, H. et al. A supercompressible, elastic, and bendable carbon aerogel with ultrasensitive detection limits for compression strain, pressure, and bending angle. *Adv. Mater.* **30**, 1706705 (2018).
170. Han, Z. et al. Ultralow-cost, highly sensitive, and flexible pressure sensors based on carbon black and airlaid paper for wearable electronics. *ACS Appl. Mater. Interfaces* **11**, 9b12929 (2019).
171. Liang, Z. et al. Tactile sensors: high-performance flexible tactile sensor enabling intelligent haptic perception for a soft prosthetic hand. *Adv. Mater. Technol.* **4**, 1970041 (2019).
172. Liu, Y. et al. Epidermal mechano-acoustic sensing electronics for cardiovascular diagnostics and human-machine interfaces. *Sci. Adv.* **2**, e1601185 (2016).
173. Ching, S. S. & Tan, Y. K. Spectral analysis of bowel sounds in intestinal obstruction using an electronic stethoscope. *World J. Gastroenterology* **18**, 4585 (2012).
174. Wang, F. et al. A flexible skin-mounted wireless acoustic device for bowel sounds monitoring and evaluation. *Sci. China Inf. Sci.* **62**, 202402 (2019).
175. Wang, C. et al. Monitoring of the central blood pressure waveform via a conformal ultrasonic device. *Nat. Biomed. Eng.* **2**, 687 (2018).
176. Kim, J., Campbell, A. S., de Ávila, B. E.-F. & Wang, J. Wearable biosensors for healthcare monitoring. *Nat. Biotechnol.* **37**, 389–406 (2019).
177. Mannoor, M. S. et al. Graphene-based wireless bacteria detection on tooth enamel. *Nat. Commun.* **3**, 763 (2012).
178. Kim, J. et al. Non-invasive mouthguard biosensor for continuous salivary monitoring of metabolites. *Analyst* **139**, 1632–1636 (2014).
179. Kim, J. et al. Wearable salivary uric acid mouthguard biosensor with integrated wireless electronics. *Biosens. Bioelectron.* **74**, 1061–1068 (2015).
180. Heikenfeld, J. et al. Accessing analytes in biofluids for peripheral biochemical monitoring. *Nat. Biotechnol.* **37**, 407–419 (2019).
181. Kim, J. et al. Wearable smart sensor systems integrated on soft contact lenses for wireless ocular diagnostics. *Nat. Commun.* **8**, 14997 (2017).
182. Glennon, T. et al. A wearable platform for harvesting and analysing sweat sodium content. *Electroanalysis* **28**, 1283–1289 (2016).
183. Jadoon, S. et al. Recent developments in sweat analysis and its applications. *Int. J. Anal. Chem.* **2015**, 164974 (2015).
184. Koh, A. et al. A soft, wearable microfluidic device for the capture, storage, and colorimetric sensing of sweat. *Sci. Transl. Med.* **8**, 366ra165(2016).
185. Huang, X. et al. Stretchable, wireless sensors and functional substrates for epidermal characterization of sweat. *Small* **10**, 3083–3090 (2014).
186. Nyein, H. Y. Y. et al. A wearable electrochemical platform for noninvasive simultaneous monitoring of Ca<sup>2+</sup> and pH. *ACS Nano* **10**, 7216–7224 (2016).
187. Gao, W. et al. Wearable microsensor array for multiplexed heavy metal monitoring of body fluids. *ACS Sens.* **1**, 866–874 (2016).
188. Emaminejad, S. et al. Autonomous sweat extraction and analysis applied to cystic fibrosis and glucose monitoring using a fully integrated wearable platform. *Proc. Natl Acad. Sci. USA* **114**, 4625–4630 (2017).
189. Choi, J., Kang, D., Han, S., Kim, S. B. & Rogers, J. A. Thin, soft, skin-mounted microfluidic networks with capillary bursting valves for chrono-sampling of sweat. *Adv. Healthc. Mater.* **6**, 1601355 (2017).
190. Choi, J. et al. Soft, skin-mounted microfluidic systems for measuring secretory fluidic pressures generated at the surface of the skin by eccrine sweat glands. *Lab a Chip* **17**, 2572–2580 (2017).
191. Choi, J., Ghaffari, R., Baker, L. B. & Rogers, J. A. Skin-interfaced systems for sweat collection and analytics. *Sci. Adv.* **4**, eaar3921 (2018).
192. Kim, S. B. et al. Super-absorbent polymer valves and colorimetric chemistries for time-sequenced discrete sampling and chloride analysis of sweat via skin-mounted soft microfluidics. *Small* **14**, 1703334 (2018).
193. Sekine, Y. et al. A fluorometric skin-interfaced microfluidic device and smartphone imaging module for in situ quantitative analysis of sweat chemistry. *Lab a Chip* **18**, 2178–2186 (2018).
194. Kim, S. B. et al. Soft, Skin-interfaced microfluidic systems with wireless, battery-free electronics for digital, real-time tracking of sweat loss and electrolyte composition. *Small* **14**, 1802876 (2018).
195. Bandodkar, A. J. et al. Battery-free, skin-interfaced microfluidic/electronic systems for simultaneous electrochemical, colorimetric, and volumetric analysis of sweat. *Sci. Adv.* **5**, eaav3294 (2019).
196. Reeder, J. T. et al. Waterproof, electronics-enabled, epidermal microfluidic devices for sweat collection, biomarker analysis, and thermography in aquatic settings. *Sci. Adv.* **5**, eaau6356 (2019).
197. Choi, J. et al. Soft, Skin-integrated multifunctional microfluidic systems for accurate colorimetric analysis of sweat biomarkers and temperature. *ACS Sens.* **4**, 379–388 (2019).
198. Vashist, S. K. Non-invasive glucose monitoring technology in diabetes management: A review. *Analytica Chim. Acta* **750**, 16–27 (2012).
199. Zierler, K. Whole body glucose metabolism. *Am. J. Physiol.* **276**, E409 (1999).
200. Kim, J., Campbell, A. S. & Wang, J. Wearable non-invasive epidermal glucose sensors: a review. *Talanta* **177**, 163–170 (2018).
201. Matzeu, G., Florea, L. & Diamond, D. Advances in wearable chemical sensor design for monitoring biological fluids. *Sens. Actuators B Chem.* **211**, 403–418 (2015).
202. Boyne, M. S., Silver, D. M., Kaplan, J. & Saudek, C. D. Timing of changes in interstitial and venous blood glucose measured with a continuous subcutaneous glucose sensor. *Diabetes* **52**, 2790 (2003).
203. Potts, R. O., A. Tamada, J. & J. Tierney, M. Glucose monitoring by reverse iontophoresis. *Diabetes/Metab. Res. Rev.* **18**, S49–S53 (2002).
204. Tamada, J. A., Bohannon, N. J. & Potts, R. O. Measurement of glucose in diabetic subjects using noninvasive transdermal extraction. *Nat. Med.* **1**, 1198–1201 (1995).
205. Rao, G. et al. Reverse iontophoresis: noninvasive glucose monitoring in vivo in humans. *Pharm. Res.* **12**, 1869 (1995).
206. Chen, Y., Lu, S. & Feng, X. in *2017 IEEE International Electron Devices Meeting (IEDM)*. 18.12. 11–18.12. 14 (IEEE).
207. Veisheh, O. & Langer, R. Diabetes: a smart insulin patch. *Nature* **524**, 39 (2015).
208. Wang, C., Ye, Y., Hochu, G. M., Sadeghifar, H. & Gu, Z. Enhanced cancer immunotherapy by microneedle patch-assisted delivery of anti-PD1 antibody. *Nano Lett.* **16**, 2334–2340 (2016).
209. Yu, J. et al. Microneedle-array patches loaded with hypoxia-sensitive vesicles provide fast glucose-responsive insulin delivery. *Proc. Natl Acad. Sci. USA* **112**, 8260–8265 (2015).
210. Lu, Y., Aimeetti, A. A., Langer, R. & Gu, Z. Bioresponsive materials. *Nature Reviews. Materials* **2**, 16075 (2017).
211. Yu, J. et al. Hypoxia and H<sub>2</sub>O<sub>2</sub> dual-sensitive vesicles for enhanced glucose-responsive insulin delivery. *Nano Lett.* **17**, 733–739 (2017).
212. Cai, S. et al. Review on flexible photonics/electronics integrated devices and fabrication strategy. *Sci. China Inf. Sci.* **61**, 060410 (2018).

## ACKNOWLEDGEMENTS

We gratefully acknowledge the support from the National Basic Research Program of China (Grant No. 2015CB351900) and the National Natural Science Foundation of China (Grant No. 11625207, 11320101001, and 11222220).

## AUTHOR CONTRIBUTIONS

X.F. and Y.C. conceptualized the work; Y.C., Y.C.Z., Z.W.L., Y.C., Z.Y.H. and F.L.W. collected the data and contributed to the scientific discussions and wrote the manuscript. X.F. provided overall supervision of the work.

## COMPETING INTERESTS

The authors declare no competing interests.

## ADDITIONAL INFORMATION

**Correspondence** and requests for materials should be addressed to X.F.

**Reprints and permission information** is available at <http://www.nature.com/reprints>

**Publisher's note** Springer Nature remains neutral with regard to jurisdictional claims in published maps and institutional affiliations.



**Open Access** This article is licensed under a Creative Commons Attribution 4.0 International License, which permits use, sharing, adaptation, distribution and reproduction in any medium or format, as long as you give appropriate credit to the original author(s) and the source, provide a link to the Creative Commons license, and indicate if changes were made. The images or other third party material in this article are included in the article's Creative Commons license, unless indicated otherwise in a credit line to the material. If material is not included in the article's Creative Commons license and your intended use is not permitted by statutory regulation or exceeds the permitted use, you will need to obtain permission directly from the copyright holder. To view a copy of this license, visit <http://creativecommons.org/licenses/by/4.0/>.

© The Author(s) 2020